

CHAPTER 1

MULTIFERROICS AND METAMATERIALS

This chapter is a literature review for the optical properties of multiferroics and other groups of bi-anisotropic optical materials, such as metamaterials. The main source of information is from recent review articles References [1,2,3,4,5].

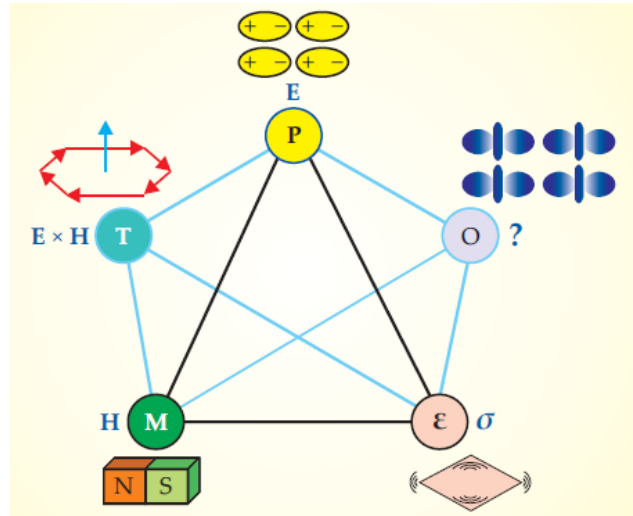


Figure 1.1 Interaction in multiferroics. The well established primary ferroic orderings: ferroelectricity, ferrromagnetizm, ferroelasticity can be switched by their conjugate electric, magnetic and stress fields, respectively. Image is from Nicola A.Spaldin, S.Cheong, R. Ramesh “Multiferroics: Past, Present and Future,” Physics today, October (2010), pp 39-43 [2].

It is always useful to have materials which allow controlling light propagation based on their unique intrinsic properties. An additional possibility to control the reflected or transmitted light by means of application of external electric and magnetic fields to such materials becomes even more important. The general class of such materials is called bi-anisotropic. There are many commonly known optical effects in bi-anisotropic medium such as polarization plane rotation, Kerr effect, Faraday effect, negative index of refraction [4,5]. This bi-anisotropic behavior can be found in materials

called multiferroics, which combine several ferroic orders, such as ferroelectric, (anti)ferromagnetic, and ferroelastic. Typical interactions in multiferroics are shown in Figure. 1.1. Either electric field E , magnetic field H , or stress σ can control the electric polarization P , magnetization M , and strain ε . Another class of bi-anisotropic materials includes man-made artificial structures, or metamaterials, which allow for independent control of electric and magnetic field components of reflected/transmitted light.

In the center of magnetoelectric effects is a magnetoelectric coupling. By representing free energy in terms of applied fields (E and H) the following expression can be obtained [Error! Bookmark not defined.]:

$$-F(E, H) = \frac{1}{2} \varepsilon_0 \varepsilon_{ij} E_i E_j + \frac{1}{2} \mu_0 \mu_{ij} H_i H_j + \alpha_{ij} E_i H_j + \frac{1}{2} \beta_{ijk} E_i H_j H_k + \frac{1}{2} \gamma_{ijk} H_i E_j E_k + \dots \quad (1.1)$$

Here ε - permittivity tensor, μ - permeability tensor, α - magnetoelectric coupling tensor, γ and further – high order of magnetoelectric coupling tensors. Terms on the RHS (from left to right) represent electrical effect from application electric field, magnetic effect from application magnetic field, electric effect from application magnetic field, magnetic effect from application electric field correspondingly and so on. To establish polarization $P_i(H_j)$ and magnetization $M_i(E_j)$, differentiation of F with respect to E_i and H_i is required:

$$\begin{aligned} P_i &= \alpha_{ij} H_j + \frac{1}{2} \beta_{ijk} H_j H_k + \dots \\ \mu_0 M_i &= \alpha_{ji} E_j + \frac{1}{2} \gamma_{ijk} E_j E_k + \dots \end{aligned} \quad (1.2)$$

It can be pointed out that for thermodynamic reasons, α_{ij} is bounded by the geometric mean of the diagonalized permittivity and permeability tensors **[Error! Bookmark not defined.]**:

$$\alpha_{ij}^2 \leq \epsilon_0 \mu_0 \epsilon_{ii} \mu_{jj} \quad (1.3)$$

Tensor α_{ij} is a second rank tensor that is a function of temperature T . It changes sign under space inversion or time reversal, and therefore is invariant under simultaneous space and time inversion. Using the definition of α_{ij} and α'_{ij} based on the free energy Equation (1.1), it is easy to assume that $\alpha^T_{ij} = \alpha'_{ij}$. As shown by Dzyaloshinsky, this relationship holds for the static case but may not necessary hold at every particular frequency for the dynamic case, where more complicated interactions of magnons and phonons are involved. This question is still under discussion in literature [6]. To comply with a general possible case, we will keep a different notation for α_{ij} and α'_{ij} tensors. ME effect exists only in materials that do not have a center of inversion and no time-inversion symmetry. In most cases, center of inversion is destroyed by electric polarization in ferroelectrics, while the time-reverse invariance is destroyed by the magnetic order or by external magnetic field. That means, ME crystals allow a simultaneous presence of magnetization (that destroys time reversal) and electric polarization (that destroys the center of inversion). The role of symmetry is extremely important in determining which crystals can display the magneto-electric effect. Crystal symmetry, for example, determines the form of each of the $\epsilon, \mu, \alpha, \beta, \gamma$ tensors. Neumann's principle states that the symmetry elements of any physical property of a crystal must include the symmetry elements of the point group of the crystal. This

principle makes clear connection between the physical properties of a crystal and the material tensor which describes those properties.

CHAPTER 2

ELECTROMAGNETIC WAVE PROPAGATION IN BI-ANISOTROPIC BULK STRUCTURES

Chapter 2 of this thesis describes the 4×4 matrix formalism applied to bulk structures, which is the most advanced approach for the light propagation problem in bi-anisotropic medium. The main references of this chapter are the original Berreman's paper [7], the Azzam's book [8] and the thesis of Paul Rogers [9,10]. In addition to the theoretical background, in this Chapter we will discuss some analytical solution of Fresnel's coefficients, which describe behavior of light when propagating through an interface between two optical media, for general bulk structures with anisotropic $\hat{\epsilon}(\omega)$, $\hat{\mu}(\omega)$ and magneto-electric interaction which characterizes by magneto-electric (ME) tensor $\hat{\alpha}(\omega)$. Also we show which components of Mueller matrix depends on ME interactions for ME tensors with different symmetries. It is a useful knowledge for measurements to determine for which sample orientation magneto-electric interaction can be observed in optical spectra and exhibit the strongest effect.

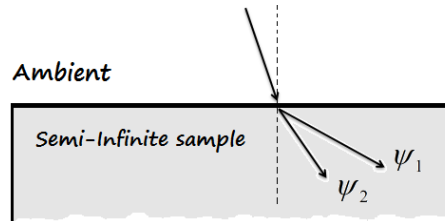


Figure 2.1 Light propagation from isotropic ambient to semi-infinite bi-anisotropic bulk structure.

2.1 Constitutive and Dispersion Relations.

We concern with structures which exhibit coupling between electric and magnetic interactions. For such a media different form of constitutive relations should be obtained in order to proper characterize wave propagation in this matter. Dzyaloshinskii obtained constitutive relations in the following form [6]:

$$\begin{aligned} D^\alpha &= \varepsilon^{\alpha\beta} E_\beta + \alpha^{\alpha\beta} H_\beta \\ B^\alpha &= \alpha^{\beta\alpha} E_\beta + \mu^{\alpha\beta} H_\beta \end{aligned} \quad (2.1)$$

Details on these equations were discussed in the section 1.2 on multiferroics in the previous chapter. Another question, which arises after all relevant relationships are written down, is how to characterize electric, magnetic and electromagnetic interactions with a few measurable quantities in the optical spectra, such as resonant frequencies, broadening, and oscillator strength. One of the most suitable approaches is Lorentz model (or simple harmonic oscillator) for dispersion relations:

$$\varepsilon(\omega) = \varepsilon_\infty + \sum_{n=1}^N \frac{S_{\varepsilon,n} \omega_{\varepsilon,0n}^2}{\omega_{\varepsilon,0n}^2 - \omega^2 - i\gamma_{\varepsilon,n}\omega} \quad (2.2)$$

$$\mu(\omega) = \mu_\infty + \sum_{n=1}^N \frac{S_{\mu,n} \omega_{\mu,0n}^2}{\omega_{\mu,0n}^2 - \omega^2 - i\gamma_{\mu,n}\omega} \quad (2.3)$$

where ω_{0n} - oscillator resonance phonon or magnon frequency or electronic transition frequency, S_n - corresponding oscillator strength, γ_n - broadening of the n^{th} excitation or electronic transition. The same is valid for treating ME interactions:

$$\alpha(\omega) = \frac{S_{me} \omega_{me,0}^2}{\omega_{me,0}^2 - \omega^2 - i\gamma_{me}\omega}; \quad \alpha(0) = S_{me}; \quad \alpha(\infty) = 0 \quad (2.4)$$

Also we will often assume that the same oscillator that appears in several $\hat{\varepsilon}$, $\hat{\mu}$, $\hat{\alpha}$, and $\hat{\xi}$ tensors has at the same frequency ω_0 and the same value of the decay parameter γ . In the figure below graphs for each type of excitation are shown. Panels (a) and (b) show real and imaginary part of electric excitation respectively, panels (c) and (d) show real and imaginary part of magnetic excitation, panel (e) and (f) show real and imaginary part of magneto-electric excitation. Parameters for each oscillator are presented in Table 2.1.

Table 2.1 Parameters for electric, magnetic and magneto-electric oscillators as described by Equations (2.2), (2.3), and (2.4).

	$\varepsilon(\omega)$	$\mu(\omega)$	$\alpha(\omega)$
Infinity value	$\varepsilon_\infty = 10$	$\mu_\infty = 1$	$\alpha_\infty = 0$
Resonant frequency	$\omega_{0,e} = 300$	$\omega_{0,\mu} = 300$	$\omega_{0,\alpha} = 300$
Strength	$S_e = 0.01$	$S_\mu = 0.01$	$S_\alpha = 0.01$
Broadening	$\gamma_e = 1$	$\gamma_\mu = 1$	$\gamma_\alpha = 1$

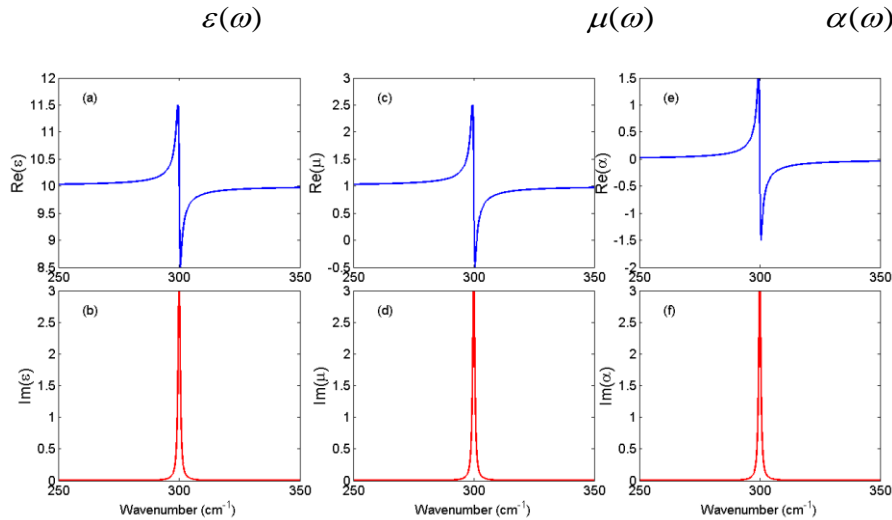


Figure 2.2 Graphs of different types of excitations: (a),(b) – electric; (c),(d) – magnetic; (e),(f) – magneto-electric. Real parts are in blue color, imaginary parts are in red color. Parameters are presented in Table 2.1.

2.2 Basics of the 4x4 Matrix Formalism

The 4×4 matrix formalism developed by Berreman [7] allow to calculate optical properties of stratified bi-anisotropic media if $\hat{\epsilon}$, $\hat{\mu}$, $\hat{\alpha}$ tensors are known. Figure 2.3 shows the optical matrix M that is composed of the $\hat{\epsilon}$, $\hat{\mu}$, $\hat{\alpha}$ tensors for a single layer with bi-anisotropic properties. For analysis of experimental data, it is always useful to have analytical solutions for transmittance and reflectance of the media as a function of frequency and angle of incidence to be able to explore phenomena like in the case of the adjusted oscillator strength matching (AOSM), total reflection, skin depth, *etc.* The schematics of the investigated experimental configuration is shown in Figure 2.4. In Berreman formalism, it is assumed that the time variation of fields are harmonic and given by $e^{i\omega t}$, the direction of stratification coincides with the positive direction of the z -axis, there is no \vec{k}_y wave vector component of incident light and structures are homogeneous along x . The theory utilizes the fact that parallel components of the fields are continuous through out the medium (no surface charges, no surface currents).

$$\begin{array}{c}
 \hat{\alpha}(\omega), \hat{\alpha}'(\omega) \\
 \downarrow \\
 \hat{\epsilon}(\omega) \longrightarrow \text{Optical Matrix} \longleftarrow \hat{\mu}(\omega) \\
 \updownarrow \\
 \begin{pmatrix} \vec{D} \\ \vec{B} \end{pmatrix} = \begin{pmatrix} \hat{\epsilon} & \hat{\alpha} \\ \hat{\alpha}' & \hat{\mu} \end{pmatrix} \begin{pmatrix} \vec{E} \\ \vec{H} \end{pmatrix}
 \end{array}$$

Figure 2.3 Constitutive relations for bi-anisotropic structures. Sample can be described by permittivity $\hat{\epsilon}(\omega)$, permeability $\hat{\mu}(\omega)$ and ME $\hat{\alpha}(\omega)$ tensors. \vec{D} and \vec{B} relate to \vec{E} and \vec{H} by means of optical matrix.

The advantage of Berreman's formalism is that it deals with the first order Maxwell's equations which allow to easily incorporate the ME tensors. Note that in

addition to the Berreman's approach, there are some other ways to investigate electromagnetic wave propagation but they rely on the same physical principles though math is a bit different. In comparison, the Yeh's [11] formalism deals with polarization eigenmodes, giving a more clear physical interpretation of boundary conditions, but this approach seems to be more difficult to describe magneto-electric activity and optical activity. We chose Berreman's approach as an established one which allows to obtain all required results for our research.

It is instructive to show derivation of Berreman's matrix wave equation and discuss application of boundary conditions to have clear understanding of incorporating ME effect into structure's interactions.

$$\begin{aligned}
 \vec{D} &= \hat{\epsilon} \vec{E} + \hat{\alpha} \vec{H} \\
 \vec{B} &= \hat{\alpha}' \vec{E} + \hat{\mu} \vec{H} \\
 \begin{pmatrix} \vec{D} \\ \vec{B} \end{pmatrix} &= \begin{pmatrix} \hat{\epsilon} & \hat{\alpha} \\ \hat{\alpha}' & \hat{\mu} \end{pmatrix} \begin{pmatrix} \vec{E} \\ \vec{H} \end{pmatrix}
 \end{aligned} \tag{2.5}$$

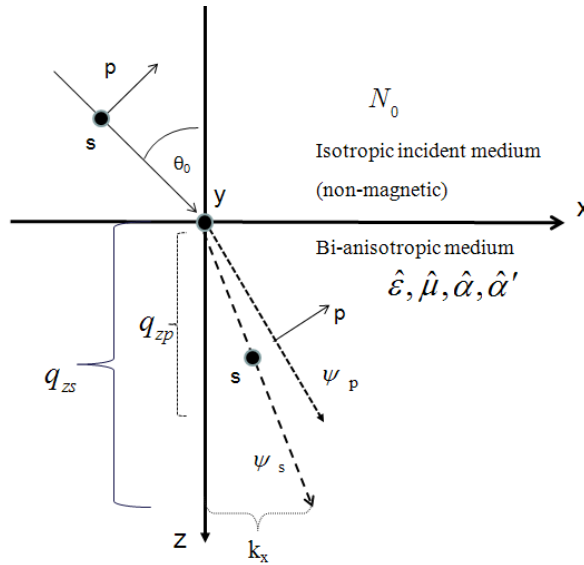


Figure 2.4 Axis orientation and schematics of wave propagation.

For simplicity we assume that our laboratory x - y - z axes coincide with the symmetry axes of the sample. Such convention determines the diagonal form of both, dielectric permittivity tensor and magnetic permeability tensors. Schematic of the axes notation is shown in Figure 2.4. When this condition does not hold we should rotate our optical axes, transforming correspondingly our optical matrix and it won't have diagonal form anymore. Constitutive relations can be written in the following form:

$$\begin{pmatrix} D_x \\ D_y \\ D_z \\ B_x \\ B_y \\ B_z \end{pmatrix} = \begin{pmatrix} \varepsilon_{xx} & 0 & 0 & \alpha_{xx} & \alpha_{xy} & \alpha_{xz} \\ 0 & \varepsilon_{yy} & 0 & \alpha_{yx} & \alpha_{yy} & \alpha_{yz} \\ 0 & 0 & \varepsilon_{zz} & \alpha_{zx} & \alpha_{zy} & \alpha_{zz} \\ \alpha_{xx}^* & \alpha_{yx}^* & \alpha_{zx}^* & \mu_{xx} & 0 & 0 \\ \alpha_{xy}^* & \alpha_{yy}^* & \alpha_{zy}^* & 0 & \mu_{yy} & 0 \\ \alpha_{xz}^* & \alpha_{yz}^* & \alpha_{zz}^* & 0 & 0 & \mu_{zz} \end{pmatrix} \begin{pmatrix} E_x \\ E_y \\ E_z \\ H_x \\ H_y \\ H_z \end{pmatrix} \quad (2.6)$$

It should be noted that a low-left part of optical matrix $\hat{\alpha}'$ is a conjugate transpose of $\hat{\alpha}$: $\hat{\alpha}' = \hat{\alpha}^\dagger$. In the following discussion we focus on the cases when non-zero components of ME tensor are $\alpha_{xx}, \alpha_{yy}, \alpha_{zz}, \alpha_{yx} = -\alpha_{xy}, \alpha_{yz} = -\alpha_{zy}, \alpha_{zx} = -\alpha_{xz}$ which corresponds to most common crystal structure.

Let's write down Maxwell's equations (in the general case of ME tensor each field component is a function of others):

$$\begin{cases} \nabla \times \vec{E} = -\frac{\partial \vec{B}}{\partial t} \\ \nabla \times \vec{H} = \frac{\partial \vec{D}}{\partial t} \end{cases} \quad (2.7)$$

It is useful to represent *curl* vector as a matrix and note that our conditions assume that there is no \vec{k}_y component of wave vector and our material is homogeneous as the result

$\frac{\partial}{\partial y}$ will bring zero and $\frac{\partial}{\partial x}$ gives us x -component of a wave vector. Full curl matrix can

be represented as in the following equation:

$$\begin{bmatrix} 0 & 0 & 0 & 0 & -\frac{\partial}{\partial z} & \frac{\partial}{\partial y} \\ 0 & 0 & 0 & \frac{\partial}{\partial z} & 0 & -\frac{\partial}{\partial x} \\ 0 & 0 & 0 & -\frac{\partial}{\partial y} & \frac{\partial}{\partial x} & 0 \\ 0 & \frac{\partial}{\partial z} & -\frac{\partial}{\partial y} & 0 & 0 & 0 \\ -\frac{\partial}{\partial z} & 0 & \frac{\partial}{\partial x} & 0 & 0 & 0 \\ \frac{\partial}{\partial y} & -\frac{\partial}{\partial x} & 0 & 0 & 0 & 0 \end{bmatrix} \begin{bmatrix} E_x \\ E_y \\ E_z \\ H_x \\ H_y \\ H_z \end{bmatrix} = \frac{1}{c} \frac{\partial}{\partial t} \begin{bmatrix} D_x \\ D_y \\ D_z \\ B_x \\ B_y \\ B_z \end{bmatrix} \quad (2.8)$$

Taking into account our discussion above and writing down constitutive relations, our matrix equation transforms to the following equation:

$$\begin{bmatrix} 0 & 0 & 0 & 0 & -\frac{\partial}{\partial z} & 0 \\ 0 & 0 & 0 & \frac{\partial}{\partial z} & 0 & ik_x \\ 0 & 0 & 0 & 0 & -ik_x & 0 \\ 0 & \frac{\partial}{\partial z} & 0 & 0 & 0 & 0 \\ -\frac{\partial}{\partial z} & 0 & -ik_x & 0 & 0 & 0 \\ 0 & ik_x & 0 & 0 & 0 & 0 \end{bmatrix} \begin{bmatrix} E_x \\ E_y \\ E_z \\ H_x \\ H_y \\ H_z \end{bmatrix} = \frac{1}{c} \begin{pmatrix} \hat{\varepsilon} & \hat{\alpha} \\ \hat{\alpha}' & \hat{\mu} \end{pmatrix} \frac{\partial}{\partial t} \begin{bmatrix} E_x \\ E_y \\ E_z \\ H_x \\ H_y \\ H_z \end{bmatrix} \quad (2.9)$$

Most general view can be shown as:

$$\begin{bmatrix} 0 & 0 & 0 & 0 & -\frac{\partial}{\partial z} & 0 \\ 0 & 0 & 0 & \frac{\partial}{\partial z} & 0 & ik_x \\ 0 & 0 & 0 & 0 & -ik_x & 0 \\ 0 & \frac{\partial}{\partial z} & 0 & 0 & 0 & 0 \\ -\frac{\partial}{\partial z} & 0 & -ik_x & 0 & 0 & 0 \\ 0 & ik_x & 0 & 0 & 0 & 0 \end{bmatrix} \begin{bmatrix} E_x \\ E_y \\ E_z \\ H_x \\ H_y \\ H_z \end{bmatrix} = \frac{1}{c} \begin{pmatrix} \varepsilon_{xx} & 0 & 0 & \alpha_{xx} & \alpha_{xy} & \alpha_{xz} \\ 0 & \varepsilon_{yy} & 0 & \alpha_{yx} & \alpha_{yy} & \alpha_{yz} \\ 0 & 0 & \varepsilon_{zz} & \alpha_{zx} & \alpha_{zy} & \alpha_{zz} \\ \alpha'_{xx} & \alpha'_{yx} & \alpha'_{zx} & \mu_{xx} & 0 & 0 \\ \alpha'_{xy} & \alpha'_{yy} & \alpha'_{zy} & 0 & \mu_{yy} & 0 \\ \alpha'_{xz} & \alpha'_{yz} & \alpha'_{zz} & 0 & 0 & \mu_{zz} \end{pmatrix} \frac{\partial}{\partial t} \begin{bmatrix} E_x \\ E_y \\ E_z \\ H_x \\ H_y \\ H_z \end{bmatrix} \quad (2.10)$$

Looking carefully at the *curl* matrix it should be noted that there is no $\frac{\partial}{\partial z}$ dependencies in third and sixth column. That means we can express E_z and H_z components in terms of E_x, E_y, H_x, H_y . Our “reduced” equation looks like:

$$\frac{\partial}{\partial z} \begin{pmatrix} E_x \\ E_y \\ H_x \\ H_y \end{pmatrix} = i \frac{\omega}{c} \begin{pmatrix} \Delta_{11} & \Delta_{12} & \Delta_{13} & \Delta_{14} \\ \Delta_{21} & \Delta_{22} & \Delta_{23} & \Delta_{24} \\ \Delta_{31} & \Delta_{32} & \Delta_{33} & \Delta_{34} \\ \Delta_{41} & \Delta_{42} & \Delta_{43} & \Delta_{44} \end{pmatrix} \begin{pmatrix} E_x \\ E_y \\ H_x \\ H_y \end{pmatrix} \quad (2.11)$$

Calculation of $\tilde{\Delta}$ matrix elements can be found in original Berreman’s paper [7]. Though

Berreman used $\begin{pmatrix} E_x \\ H_y \\ E_y \\ -H_x \end{pmatrix}$ basis (and calculated $\tilde{\Delta}$ elements in this basis), we use $\begin{pmatrix} E_x \\ E_y \\ H_x \\ H_y \end{pmatrix}$

basis. It is not hard to get expressions for $\tilde{\Delta}$ elements in our basis by slightly

modifying Berreman's matrix as shown in Figure 2.5. There is no principle difference which basis to choose, but it is more important to work with \vec{E} and \vec{H} because their

$$\begin{array}{ccc}
 \text{Berreman's} & & \text{Our work} \\
 \left(\begin{array}{cccc} \Delta_{11} & \Delta_{12} & \Delta_{13} & \Delta_{14} \\ \Delta_{21} & \Delta_{22} & \Delta_{23} & \Delta_{24} \\ \Delta_{31} & \Delta_{32} & \Delta_{33} & \Delta_{34} \\ \Delta_{41} & \Delta_{42} & \Delta_{43} & \Delta_{44} \end{array} \right) & \xrightarrow{\text{transformation}} & \left(\begin{array}{cccc} \Delta_{11} & \Delta_{13} & -\Delta_{14} & \Delta_{12} \\ \Delta_{31} & \Delta_{33} & -\Delta_{34} & \Delta_{32} \\ -\Delta_{41} & -\Delta_{43} & \Delta_{44} & -\Delta_{42} \\ \Delta_{21} & \Delta_{23} & -\Delta_{24} & \Delta_{22} \end{array} \right) \\
 \left(\begin{array}{c} E_x \\ H_y \\ E_y \\ -H_x \end{array} \right) & & \left(\begin{array}{c} E_x \\ E_y \\ H_x \\ H_y \end{array} \right)
 \end{array}$$

Figure 2.5 Transformation between different bases

tangential components are continuous through interfaces which as was shown earlier lay in the xy -plane.

Finally one arrives to 4x4 matrix wave equation (we use matrix on the right in Figure 2.5 but we rename components of $\tilde{\Delta}$):

$$\frac{\partial}{\partial z} \begin{pmatrix} E_x \\ E_y \\ H_x \\ H_y \end{pmatrix} = i \frac{\omega}{c} \begin{pmatrix} \Delta_{11} & \Delta_{12} & \Delta_{13} & \Delta_{14} \\ \Delta_{21} & \Delta_{22} & \Delta_{23} & \Delta_{24} \\ \Delta_{31} & \Delta_{32} & \Delta_{33} & \Delta_{34} \\ \Delta_{41} & \Delta_{42} & \Delta_{43} & \Delta_{44} \end{pmatrix} \begin{pmatrix} E_x \\ E_y \\ H_x \\ H_y \end{pmatrix}, \quad (2.12)$$

or in a more compact form:

$$\frac{\partial \psi}{\partial z} = i \frac{\omega}{c} \tilde{\Delta} \psi \quad (2.13)$$

For our discussion about wave propagation in the bulk samples we do not need to solve Equation (2.13). It's enough to solve eigenvalue, eigenvector problem for substrate's $\tilde{\Delta}$ matrix. Further treatment of the Berreman's wave equation will be continued in the chapter on electromagnetic wave propagation in bi-anisotropic multilayer systems.

Because we assume that our structures are homogeneous along z , LHS of the Equation (2.12) yields ik_z multiplier in front of ψ vector. We can rewrite wave equation

into the form below, where q_z is an effective refraction index in the z -direction and

corresponds to the z -component of wave vector as $q_z = \frac{ck_z}{\omega}$.

$$\begin{pmatrix} \Delta_{11} & \Delta_{12} & \Delta_{13} & \Delta_{14} \\ \Delta_{21} & \Delta_{22} & \Delta_{23} & \Delta_{24} \\ \Delta_{31} & \Delta_{32} & \Delta_{33} & \Delta_{34} \\ \Delta_{41} & \Delta_{42} & \Delta_{43} & \Delta_{44} \end{pmatrix} \begin{pmatrix} E_x(0) \\ E_y(0) \\ H_x(0) \\ H_y(0) \end{pmatrix} = q_z \begin{pmatrix} E_x(0) \\ E_y(0) \\ H_x(0) \\ H_y(0) \end{pmatrix}, \quad (2.14)$$

where we consider field's components at the interface between ambient and structure. For getting analytical solutions it is nice to construct transfer matrix T which relates incident and reflected components to transmitted ones of propagating wave. We desire to have relationship in the form:

$$\begin{pmatrix} E_{is} \\ E_{rs} \\ E_{ip} \\ E_{rp} \end{pmatrix} = T \begin{pmatrix} E_{ts} \\ 0 \\ E_{tp} \\ 0 \end{pmatrix} = \begin{pmatrix} T_{11} & T_{12} & T_{13} & T_{14} \\ T_{21} & T_{22} & T_{23} & T_{24} \\ T_{31} & T_{32} & T_{33} & T_{34} \\ T_{41} & T_{42} & T_{43} & T_{44} \end{pmatrix} \begin{pmatrix} E_{ts} \\ 0 \\ E_{tp} \\ 0 \end{pmatrix} \quad (2.15)$$

Fresnel's coefficient could be found easily from this equation:

$$\begin{aligned} r_{pp} &= \frac{T_{11}T_{43} - T_{13}T_{41}}{T_{11}T_{33} - T_{13}T_{31}} & t_{pp} &= \frac{T_{11}}{T_{11}T_{33} - T_{13}T_{31}} \\ r_{sp} &= \frac{T_{11}T_{23} - T_{13}T_{21}}{T_{11}T_{33} - T_{13}T_{31}} & t_{sp} &= -\frac{T_{13}}{T_{11}T_{33} - T_{13}T_{31}} \\ r_{ss} &= \frac{T_{21}T_{33} - T_{23}T_{31}}{T_{11}T_{33} - T_{13}T_{31}} & t_{ss} &= \frac{T_{33}}{T_{11}T_{33} - T_{13}T_{31}} \\ r_{ps} &= \frac{T_{33}T_{41} - T_{31}T_{43}}{T_{11}T_{33} - T_{13}T_{31}} & t_{ps} &= -\frac{T_{31}}{T_{11}T_{33} - T_{13}T_{31}}. \end{aligned} \quad (2.16)$$

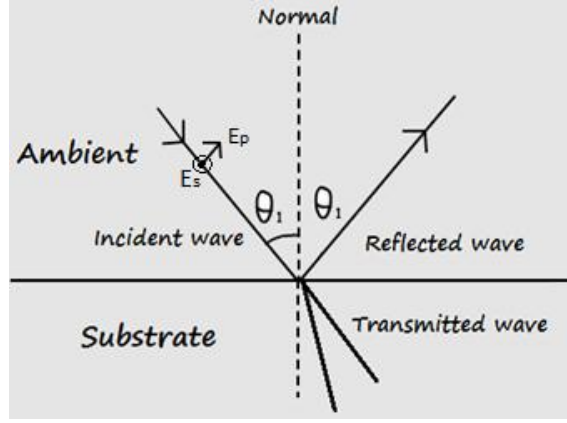


Figure 2.6 Fields near the ambient-substrate interface. z -axis is along vertical line going down, y -axis is perpendicular out of the page and x -axis is along horizontal line with positive direction to the right.

What one needs is to construct matrices which project transmitted waves on xy -plane and project xy -components on initial and reflected waves. Projecting E_p, E_s components of incident and reflected waves on the interface and using relationship between H and E for isotropic medium we get following dependencies for incident light:

$$\begin{pmatrix} E_x \\ E_y \\ H_x \\ H_y \end{pmatrix}_i = \begin{pmatrix} \cos \theta_0 E_{ip} \\ E_{is} \\ -N_0 \cos \theta_0 E_{is} \\ N_0 E_{ip} \end{pmatrix} \quad (2.17)$$

for reflected light:

$$\begin{pmatrix} E_x \\ E_y \\ H_x \\ H_y \end{pmatrix}_r = \begin{pmatrix} -\cos \theta_0 E_{rp} \\ E_{rs} \\ N_0 \cos \theta_0 E_{rs} \\ N_0 E_{rp} \end{pmatrix}. \quad (2.18)$$

Total projection on the xy -plane:

$$\begin{pmatrix} E_x \\ E_y \\ H_x \\ H_y \end{pmatrix} = \begin{pmatrix} \cos \theta_0 E_{ip} \\ E_{is} \\ -N_0 \cos \theta_0 E_{is} \\ N_0 E_{ip} \end{pmatrix} + \begin{pmatrix} -\cos \theta_0 E_{rp} \\ E_{rs} \\ N_0 \cos \theta_0 E_{rs} \\ N_0 E_{rp} \end{pmatrix} \quad (2.19)$$

or if we reshape RHS of Equation (2.19) we get:

$$\begin{pmatrix} E_x \\ E_y \\ H_x \\ H_y \end{pmatrix} = \begin{pmatrix} 0 & 0 & \cos \theta_0 & -\cos \theta_0 \\ 1 & 1 & 0 & 0 \\ -N_0 \cos \theta_0 & N_0 \cos \theta_0 & 0 & 0 \\ 0 & 0 & N_0 & N_0 \end{pmatrix} \begin{pmatrix} E_{is} \\ E_{rs} \\ E_{ip} \\ E_{rp} \end{pmatrix} \quad (2.20)$$

In order to get p and s components along we multiply both parts on the inverse matrix in the RHS of Equation (2.20):

$$\begin{pmatrix} 0 & 0 & \cos \theta_0 & -\cos \theta_0 \\ 1 & 1 & 0 & 0 \\ -N_0 \cos \theta_0 & N_0 \cos \theta_0 & 0 & 0 \\ 0 & 0 & N_0 & N_0 \end{pmatrix}^{-1} \begin{pmatrix} E_x \\ E_y \\ H_x \\ H_y \end{pmatrix} = \begin{pmatrix} E_{is} \\ E_{rs} \\ E_{ip} \\ E_{rp} \end{pmatrix} \quad (2.21)$$

and finally following Shubert [12] we obtain matrix L_{in} which project x,y -components of the incident and reflected waves on p,s -components:

$$\begin{pmatrix} E_{is} \\ E_{rs} \\ E_{ip} \\ E_{rp} \end{pmatrix} = L_{in} \begin{pmatrix} E_x \\ E_y \\ H_x \\ H_y \end{pmatrix} = \frac{1}{2} \begin{pmatrix} 0 & 1 & -\frac{1}{N_0 \cos \theta_i} & 0 \\ 0 & 1 & \frac{1}{N_0 \cos \theta_i} & 0 \\ \frac{1}{\cos \theta_i} & 0 & 0 & \frac{1}{N_0} \\ -\frac{1}{\cos \theta_i} & 0 & 0 & \frac{1}{N_0} \end{pmatrix} \begin{pmatrix} E_x \\ E_y \\ H_x \\ H_y \end{pmatrix} \quad (2.22)$$

Before calculating another matrix which projects the transmitted waves on the xy -plane, let's review Azzam's method of solving wave propagation in bulk materials problem. As we pointed out earlier, in Equation (2.22) a simple relationship can be

established between incident and reflected waves and their projections on the xy -plane. We assume that our media is bi-anisotropic in general case and then it's sufficient to assume that propagating waves inside bulk structure will be nothing but linear combination of eigenvectors which corresponds to positive real part eigenvalues (condition for existing only two transmitted waves). This kind of relationship has the form:

$$\begin{cases} (E_{ip} - E_{rp}) \cos \theta_0 = C_1 \psi_{11} + C_2 \psi_{12} \\ N_0 (E_{ip} + E_{rp}) = C_1 \psi_{21} + C_2 \psi_{22} \\ (E_{is} + E_{rs}) = C_1 \psi_{31} + C_2 \psi_{32} \\ N_0 (E_{is} - E_{rs}) = C_1 \psi_{41} + C_2 \psi_{42} \end{cases} \quad (2.23)$$

After defining boundary conditions we can introduce transmission coefficients vector

$C = \begin{pmatrix} C_1 \\ C_2 \end{pmatrix}$ and rewriting our initial system of equations into more useful form we obtain:

$$\begin{cases} C = S_1 (E_i - E_r) \\ C = S_2 (E_i + E_r) \end{cases} \quad (2.24)$$

Where S_1 and S_2 are defined by the following equations:

$$\begin{aligned} S_1 &= \cos \theta_0 \begin{pmatrix} \psi_{11} & \psi_{12} \\ \frac{\psi_{41}}{N_0} & \frac{\psi_{42}}{N_0} \end{pmatrix}^{-1} \\ S_2 &= \begin{pmatrix} \frac{\psi_{21}}{N_0} & \frac{\psi_{22}}{N_0} \\ \psi_{31} & \psi_{32} \end{pmatrix}^{-1} \end{aligned} \quad (2.25)$$

Finally we get Fresnel's coefficients:

$$\begin{aligned}
R &= \begin{pmatrix} r_{pp} & r_{ps} \\ r_{sp} & r_{ss} \end{pmatrix} = (S_1 + S_2)^{-1}(S_1 - S_2) \\
T &= \begin{pmatrix} t_{pp} & t_{ps} \\ t_{sp} & t_{ss} \end{pmatrix} = S_2(I + R)
\end{aligned} \tag{2.26}$$

The disadvantage of such a method is a calculating inverse matrices several times. Shubert [12] proposed slightly different approach. We want to construct matrix which project transmitted waves on xy -plane. Let's call it L_{out} . Then we have

$$\begin{pmatrix} E_x \\ E_y \\ H_x \\ H_y \end{pmatrix} = L_{out} \begin{pmatrix} E_{ts} \\ 0 \\ E_{ps} \\ 0 \end{pmatrix} \tag{2.27}$$

From the system Equation (2.23) it's clear that

$$\begin{pmatrix} E_x \\ E_y \\ H_x \\ H_y \end{pmatrix} = E_{ts} \begin{pmatrix} \psi_{11}^{sub} \\ \psi_{21}^{sub} \\ \psi_{31}^{sub} \\ \psi_{41}^{sub} \end{pmatrix} + E_{ps} \begin{pmatrix} \psi_{12}^{sub} \\ \psi_{22}^{sub} \\ \psi_{32}^{sub} \\ \psi_{42}^{sub} \end{pmatrix} = \begin{pmatrix} \psi_{11}^{sub} & 0 & \psi_{12}^{sub} & 0 \\ \psi_{21}^{sub} & 0 & \psi_{22}^{sub} & 0 \\ \psi_{31}^{sub} & 0 & \psi_{32}^{sub} & 0 \\ \psi_{41}^{sub} & 0 & \psi_{42}^{sub} & 0 \end{pmatrix} \begin{pmatrix} E_{ts} \\ 0 \\ E_{tp} \\ 0 \end{pmatrix} \tag{2.28}$$

where ψ_{ij}^{sub} are the substrate's $\tilde{\Lambda}$ matrix eigenvectors components. As a small remark: when treating semi-infinite bulk structures we simply call it substrates because algorithms are similar to that for a multilayer structure on semi-infinite anisotropic substrate. Eigenvector components of semi-infinite bulk structures we call substrate eigenvector components ψ_{ij}^{sub} . So our L_{out} matrix has the form:

$$L_{out} = \begin{pmatrix} \psi_{11}^{sub} & 0 & \psi_{12}^{sub} & 0 \\ \psi_{21}^{sub} & 0 & \psi_{22}^{sub} & 0 \\ \psi_{31}^{sub} & 0 & \psi_{32}^{sub} & 0 \\ \psi_{41}^{sub} & 0 & \psi_{42}^{sub} & 0 \end{pmatrix} \tag{2.29}$$

Now we can write down transfer matrix T:

$$T = L_{in}L_{out} = \frac{1}{2} \begin{pmatrix} 0 & 1 & -\frac{1}{N_0 \cos \theta_i} & 0 \\ 0 & 1 & \frac{1}{N_0 \cos \theta_i} & 0 \\ \frac{1}{\cos \theta_i} & 0 & 0 & \frac{1}{N_0} \\ -\frac{1}{\cos \theta_i} & 0 & 0 & \frac{1}{N_0} \end{pmatrix} \begin{pmatrix} \psi_{11}^{sub} & 0 & \psi_{12}^{sub} & 0 \\ \psi_{21}^{sub} & 0 & \psi_{22}^{sub} & 0 \\ \psi_{31}^{sub} & 0 & \psi_{32}^{sub} & 0 \\ \psi_{41}^{sub} & 0 & \psi_{42}^{sub} & 0 \end{pmatrix} \quad (2.30)$$

And finally we get explicit formula of Equation (2.30) from which Fresnel's coefficients can be obtained in analytical form. The only thing left is to calculate corresponding eigenvectors of transmitted waves. We consider several symmetries of ME tensor which more often occurs in real materials to simplify our calculation and then we determine which Mueller matrix components depends on ME oscillators.

$$\begin{pmatrix} E_{is} \\ E_{rs} \\ E_{ip} \\ E_{rp} \end{pmatrix} = T \begin{pmatrix} E_{ts} \\ 0 \\ E_{tp} \\ 0 \end{pmatrix} = \begin{pmatrix} T_{11} & T_{12} & T_{13} & T_{14} \\ T_{21} & T_{22} & T_{23} & T_{24} \\ T_{31} & T_{32} & T_{33} & T_{34} \\ T_{41} & T_{42} & T_{43} & T_{44} \end{pmatrix} \begin{pmatrix} E_{ts} \\ 0 \\ E_{tp} \\ 0 \end{pmatrix} = \begin{pmatrix} \frac{\psi_{21}^{sub}}{2} - \frac{\psi_{31}^{sub}}{2N_0 \cos \theta_0} & 0 & \frac{\psi_{22}^{sub}}{2} - \frac{\psi_{32}^{sub}}{2N_0 \cos \theta_0} & 0 \\ \frac{\psi_{21}^{sub}}{2} + \frac{\psi_{31}^{sub}}{2N_0 \cos \theta_0} & 0 & \frac{\psi_{22}^{sub}}{2} + \frac{\psi_{32}^{sub}}{2N_0 \cos \theta_0} & 0 \\ \frac{\psi_{41}^{sub}}{2N_0} + \frac{\psi_{11}^{sub}}{2 \cos \theta_0} & 0 & \frac{\psi_{42}^{sub}}{2N_0} + \frac{\psi_{12}^{sub}}{2 \cos \theta_0} & 0 \\ \frac{\psi_{41}^{sub}}{2N_0} - \frac{\psi_{11}^{sub}}{2 \cos \theta_0} & 0 & \frac{\psi_{42}^{sub}}{2N_0} - \frac{\psi_{12}^{sub}}{2 \cos \theta_0} & 0 \end{pmatrix} \begin{pmatrix} E_{ts} \\ 0 \\ E_{tp} \\ 0 \end{pmatrix} \quad \text{Displa}$$

Fresnel's coefficients for general bulk bi-anisotropic structures with isotropic ambient (coefficients shown as a functions of the eigenvectors components):

$$r_{pp} = \frac{(\frac{\psi_{21}^{sub}}{2} - \frac{\psi_{31}^{sub}}{2N_0 \cos \theta_0})(\frac{\psi_{42}^{sub}}{2N_0} - \frac{\psi_{12}^{sub}}{2 \cos \theta_0}) - (\frac{\psi_{41}^{sub}}{2N_0} - \frac{\psi_{11}^{sub}}{2 \cos \theta_0})(\frac{\psi_{22}^{sub}}{2} - \frac{\psi_{32}^{sub}}{2N_0 \cos \theta_0})}{(\frac{\psi_{21}^{sub}}{2} - \frac{\psi_{31}^{sub}}{2N_0 \cos \theta_0})(\frac{\psi_{42}^{sub}}{2N_0} + \frac{\psi_{12}^{sub}}{2 \cos \theta_0}) - (\frac{\psi_{41}^{sub}}{2N_0} + \frac{\psi_{11}^{sub}}{2 \cos \theta_0})(\frac{\psi_{22}^{sub}}{2} - \frac{\psi_{32}^{sub}}{2N_0 \cos \theta_0})} \quad (2.32)$$

$$r_{sp} = \frac{(\frac{\psi_{21}^{sub}}{2} - \frac{\psi_{31}^{sub}}{2N_0 \cos \theta_0})(\frac{\psi_{22}^{sub}}{2} + \frac{\psi_{32}^{sub}}{2N_0 \cos \theta_0}) - (\frac{\psi_{21}^{sub}}{2} + \frac{\psi_{31}^{sub}}{2N_0 \cos \theta_0})(\frac{\psi_{22}^{sub}}{2} - \frac{\psi_{32}^{sub}}{2N_0 \cos \theta_0})}{(\frac{\psi_{21}^{sub}}{2} - \frac{\psi_{31}^{sub}}{2N_0 \cos \theta_0})(\frac{\psi_{42}^{sub}}{2N_0} + \frac{\psi_{12}^{sub}}{2 \cos \theta_0}) - (\frac{\psi_{41}^{sub}}{2N_0} + \frac{\psi_{11}^{sub}}{2 \cos \theta_0})(\frac{\psi_{22}^{sub}}{2} - \frac{\psi_{32}^{sub}}{2N_0 \cos \theta_0})} \quad (2.33)$$

$$r_{ps} = \frac{(\frac{\psi_{41}^{sub}}{2N_0} - \frac{\psi_{11}^{sub}}{2\cos\theta_0})(\frac{\psi_{42}^{sub}}{2N_0} + \frac{\psi_{12}^{sub}}{2\cos\theta_0}) - (\frac{\psi_{41}^{sub}}{2N_0} + \frac{\psi_{11}^{sub}}{2\cos\theta_0})(\frac{\psi_{42}^{sub}}{2N_0} - \frac{\psi_{12}^{sub}}{2\cos\theta_0})}{(\frac{\psi_{21}^{sub}}{2} - \frac{\psi_{31}^{sub}}{2N_0\cos\theta_0})(\frac{\psi_{42}^{sub}}{2N_0} + \frac{\psi_{12}^{sub}}{2\cos\theta_0}) - (\frac{\psi_{41}^{sub}}{2N_0} + \frac{\psi_{11}^{sub}}{2\cos\theta_0})(\frac{\psi_{22}^{sub}}{2} - \frac{\psi_{32}^{sub}}{2N_0\cos\theta_0})} \quad (2.34)$$

$$r_{ss} = \frac{(\frac{\psi_{21}^{sub}}{2} + \frac{\psi_{31}^{sub}}{2N_0\cos\theta_0})(\frac{\psi_{42}^{sub}}{2N_0} + \frac{\psi_{12}^{sub}}{2\cos\theta_0}) - (\frac{\psi_{41}^{sub}}{2N_0} + \frac{\psi_{11}^{sub}}{2\cos\theta_0})(\frac{\psi_{22}^{sub}}{2} + \frac{\psi_{32}^{sub}}{2N_0\cos\theta_0})}{(\frac{\psi_{21}^{sub}}{2} - \frac{\psi_{31}^{sub}}{2N_0\cos\theta_0})(\frac{\psi_{42}^{sub}}{2N_0} + \frac{\psi_{12}^{sub}}{2\cos\theta_0}) - (\frac{\psi_{41}^{sub}}{2N_0} + \frac{\psi_{11}^{sub}}{2\cos\theta_0})(\frac{\psi_{22}^{sub}}{2} - \frac{\psi_{32}^{sub}}{2N_0\cos\theta_0})} \quad (2.35)$$

$$t_{pp} = \frac{\frac{\psi_{21}^{sub}}{2} - \frac{\psi_{31}^{sub}}{2N_0\cos\theta_0}}{(\frac{\psi_{21}^{sub}}{2} - \frac{\psi_{31}^{sub}}{2N_0\cos\theta_0})(\frac{\psi_{42}^{sub}}{2N_0} + \frac{\psi_{12}^{sub}}{2\cos\theta_0}) - (\frac{\psi_{41}^{sub}}{2N_0} + \frac{\psi_{11}^{sub}}{2\cos\theta_0})(\frac{\psi_{22}^{sub}}{2} - \frac{\psi_{32}^{sub}}{2N_0\cos\theta_0})} \quad (2.36)$$

$$t_{sp} = -\frac{\frac{\psi_{22}^{sub}}{2} - \frac{\psi_{32}^{sub}}{2N_0\cos\theta_0}}{(\frac{\psi_{21}^{sub}}{2} - \frac{\psi_{31}^{sub}}{2N_0\cos\theta_0})(\frac{\psi_{42}^{sub}}{2N_0} + \frac{\psi_{12}^{sub}}{2\cos\theta_0}) - (\frac{\psi_{41}^{sub}}{2N_0} + \frac{\psi_{11}^{sub}}{2\cos\theta_0})(\frac{\psi_{22}^{sub}}{2} - \frac{\psi_{32}^{sub}}{2N_0\cos\theta_0})} \quad (2.37)$$

$$t_{ps} = -\frac{\frac{\psi_{41}^{sub}}{2N_0} - \frac{\psi_{11}^{sub}}{2\cos\theta_0}}{(\frac{\psi_{21}^{sub}}{2} - \frac{\psi_{31}^{sub}}{2N_0\cos\theta_0})(\frac{\psi_{42}^{sub}}{2N_0} + \frac{\psi_{12}^{sub}}{2\cos\theta_0}) - (\frac{\psi_{41}^{sub}}{2N_0} + \frac{\psi_{11}^{sub}}{2\cos\theta_0})(\frac{\psi_{22}^{sub}}{2} - \frac{\psi_{32}^{sub}}{2N_0\cos\theta_0})} \quad (2.38)$$

$$t_{ss} = \frac{\frac{\psi_{42}^{sub}}{2N_0} - \frac{\psi_{12}^{sub}}{2\cos\theta_0}}{(\frac{\psi_{21}^{sub}}{2} - \frac{\psi_{31}^{sub}}{2N_0\cos\theta_0})(\frac{\psi_{42}^{sub}}{2N_0} + \frac{\psi_{12}^{sub}}{2\cos\theta_0}) - (\frac{\psi_{41}^{sub}}{2N_0} + \frac{\psi_{11}^{sub}}{2\cos\theta_0})(\frac{\psi_{22}^{sub}}{2} - \frac{\psi_{32}^{sub}}{2N_0\cos\theta_0})}, \quad (2.39)$$

ψ_{ij}^{sub} calculated for some certain cases are available for download online in the form of

MatLab m-files which are located at <http://web.njit.edu/~sirenko/EllipsNJIT/index1.htm>.

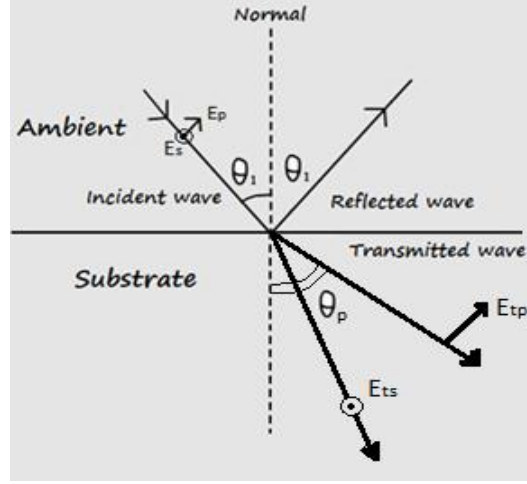


Figure 2.7 Decoupled E_{ip} and E_{is} wave propagating inside substrate.

When transmitted waves are decoupled there is a more physical way to show structure of exit matrix. In this case structure of optical and $\tilde{\Delta}$ matrices look like in the following equations correspondingly.

$$M = \begin{pmatrix} \bullet & 0 & 0 & 0 & 0 & 0 \\ 0 & \bullet & 0 & 0 & 0 & 0 \\ 0 & 0 & \bullet & 0 & 0 & 0 \\ 0 & 0 & 0 & \bullet & 0 & 0 \\ 0 & 0 & 0 & 0 & \bullet & 0 \\ 0 & 0 & 0 & 0 & 0 & \bullet \end{pmatrix} \quad (2.40)$$

$$\tilde{\Delta} = \begin{pmatrix} 0 & 0 & 0 & \Delta_{14} \\ 0 & 0 & \Delta_{23} & 0 \\ 0 & \Delta_{32} & 0 & 0 \\ \Delta_{41} & 0 & 0 & 0 \end{pmatrix} \quad (2.41)$$

Let's consider separately p -polarized and s -polarized waves. Rewrite Equation (2.14) into the form and consider p -polarized light first:

$$\begin{cases} \Delta_{11}E_x + \Delta_{12}E_y + \Delta_{13}H_x + \Delta_{14}H_y = q_z E_x \\ \Delta_{21}E_x + \Delta_{22}E_y + \Delta_{23}H_x + \Delta_{24}H_y = q_z E_y \\ \Delta_{31}E_x + \Delta_{32}E_y + \Delta_{33}H_x + \Delta_{34}H_y = q_z H_x \\ \Delta_{41}E_x + \Delta_{42}E_y + \Delta_{43}H_x + \Delta_{44}H_y = q_z H_y \end{cases} \quad (2.42)$$

We assume that there is no y-component of electric field thus and substitution all off-diagonal terms of $\tilde{\Delta}$ matrix with zeroes we get:

$$\begin{cases} \Delta_{14}H_y = q_{zp} E_x \\ \Delta_{23}H_x = 0 \\ 0 = q_{zp} H_x \\ \Delta_{41}E_x = q_{zp} H_y \end{cases} \quad (2.43)$$

From firth and fourth equations from the we get following dependencies on $\tilde{\Delta}$ matrix components of fields' projections and eigenvalues:

$$H_x = 0; H_y = \frac{q_{zp}}{\Delta_{14}} E_x = \frac{\Delta_{41}}{q_{zp}} E_x q_{zp}^2 = \Delta_{14} \Delta_{41} \quad (2.44)$$

The same system of equations as System (2.43) can be written for s-polarized light

($E_x = 0$):

$$\begin{cases} \Delta_{14}H_y = 0 \\ \Delta_{23}H_x = q_{zs} E_y \\ \Delta_{32}E_y = q_{zs} H_x \\ 0 = q_{zs} H_y \end{cases} \quad (2.45)$$

From second and third equations from the System (2.45) we get following dependencies on $\tilde{\Delta}$ matrix components of fields' projections and eigenvalues:

$$H_y = 0; H_x = \frac{q_{zs}}{\Delta_{23}} E_y = \frac{\Delta_{32}}{q_{zs}} E_y; q_{zs}^2 = \Delta_{23} \Delta_{32} \quad (2.46)$$

From Figure 2.7 we define refracted angle $\cos \theta_p$ as $\frac{q_{zp}}{\sqrt{q_x^2 + q_{zp}^2}}$. Mode for p -polarized

light and mode for s -polarized light become as in following equations correspondently:

$$\begin{pmatrix} E_x \\ 0 \\ H_x \\ H_y \end{pmatrix}_p = \begin{pmatrix} \cos \theta_p E_{tp} \\ 0 \\ 0 \\ \frac{q_{zp}}{\Delta_{14}} \cos \theta_p E_{tp} \end{pmatrix} = \begin{pmatrix} \frac{q_{zp}}{\sqrt{q_x^2 + q_{zp}^2}} E_{tp} \\ 0 \\ 0 \\ \frac{1}{\Delta_{14}} \frac{q_{zp}^2}{\sqrt{q_x^2 + q_{zp}^2}} E_{tp} \end{pmatrix} \quad (2.47)$$

$$\begin{pmatrix} 0 \\ E_y \\ H_x \\ H_y \end{pmatrix}_s = \begin{pmatrix} 0 \\ E_{ts} \\ \frac{q_{zs}}{\Delta_{23}} E_{ts} \\ 0 \end{pmatrix} \quad (2.48)$$

Total transmitted wave has the form:

$$\begin{pmatrix} E_x \\ E_y \\ H_x \\ H_y \end{pmatrix} = \begin{pmatrix} E_x \\ 0 \\ H_x \\ H_y \end{pmatrix}_p + \begin{pmatrix} 0 \\ E_y \\ H_x \\ H_y \end{pmatrix}_s = \begin{pmatrix} \frac{q_{zp}}{\sqrt{q_x^2 + q_{zp}^2}} E_{tp} \\ E_{ts} \\ \frac{q_{zs}}{\Delta_{23}} E_{ts} \\ \frac{1}{\Delta_{14}} \frac{q_{zp}^2}{\sqrt{q_x^2 + q_{zp}^2}} E_{tp} \end{pmatrix} = \begin{pmatrix} 0 & 0 & \frac{q_{zp}}{\sqrt{q_x^2 + q_{zp}^2}} & 0 \\ 1 & 0 & 0 & 0 \\ \frac{q_{zs}}{\Delta_{23}} & 0 & 0 & 0 \\ 0 & 0 & \frac{1}{\Delta_{14}} \frac{q_{zp}^2}{\sqrt{q_x^2 + q_{zp}^2}} & 0 \end{pmatrix} \begin{pmatrix} E_{ts} \\ 0 \\ E_{tp} \\ 0 \end{pmatrix} \quad (2.49)$$

Hence out matrix for this particular case is turned to be:

$$L_{out} = \begin{pmatrix} 0 & 0 & \frac{q_{zp}}{\sqrt{q_x^2 + q_{zp}^2}} & 0 \\ 1 & 0 & 0 & 0 \\ \frac{q_{zs}}{\Delta_{23}} & 0 & 0 & 0 \\ 0 & 0 & \frac{1}{\Delta_{14}} \frac{q_{zp}^2}{\sqrt{q_x^2 + q_{zp}^2}} & 0 \end{pmatrix} \quad (2.50)$$

From practical point of view substrates are usually made from materials which are isotropic or have anisotropic permittivity tensor, so we will be using Equation (2.50) for out matrix in the next chapter on electromagnetic wave propagation in multilayer systems. Consequently, the dependence of incident, reflected and transmitted wave has the following form:

$$\begin{pmatrix} E_{ts} \\ E_{rs} \\ E_{ip} \\ E_{rp} \end{pmatrix} = L_{in} L_{out} \begin{pmatrix} E_{ts} \\ 0 \\ E_{ip} \\ 0 \end{pmatrix} = \frac{1}{2} \begin{pmatrix} 0 & 1 & -\frac{1}{N_0 \cos \theta_i} & 0 \\ 0 & 1 & \frac{1}{N_0 \cos \theta_i} & 0 \\ \frac{1}{\cos \theta_i} & 0 & 0 & \frac{1}{N_0} \\ -\frac{1}{\cos \theta_i} & 0 & 0 & \frac{1}{N_0} \end{pmatrix} \begin{pmatrix} 0 & 0 & \frac{q_{zp}}{\sqrt{q_x^2 + q_{zp}^2}} & 0 \\ 1 & 0 & 0 & 0 \\ \frac{q_{zs}}{\Delta_{23}} & 0 & 0 & 0 \\ 0 & 0 & \frac{1}{\Delta_{14}} \frac{q_{zp}^2}{\sqrt{q_x^2 + q_{zp}^2}} & 0 \end{pmatrix} \begin{pmatrix} E_{ts} \\ 0 \\ E_{ip} \\ 0 \end{pmatrix} \quad (2.51)$$

To sum up, in this part of our work we present detailed discussion of electromagnetic wave propagation in bulk materials with arbitrary symmetry using Berreman's matrix formalism. We calculated Fresnel's coefficients as a function of substrate's $\tilde{\Delta}$ matrix eigenvector components and also presented explicit view of L_{out} matrix when transmitted modes in the substrate are decoupled. In the following Sections we'll continue with the treatment of particular ME tensor symmetries and will determine which components of Mueller matrix are sensitive to ME interaction.

2.3 Fresnel's Coefficients for Materials with Certain ME Tensor Symmetry.

In this section we determine Mueller matrix components dependencies on magneto-electric interaction. First we consider a symmetry case with the off-diagonal components of the ME tensor $\hat{\alpha}$, as shown in the following optical and $\tilde{\Delta}$ matrices.

$$M = \begin{pmatrix} \varepsilon_{xx} & 0 & 0 & 0 & \alpha_{xy} & 0 \\ 0 & \varepsilon_{yy} & 0 & -\alpha_{xy} & 0 & 0 \\ 0 & 0 & \varepsilon_{zz} & 0 & 0 & 0 \\ 0 & -\alpha'_{xy} & 0 & \mu_{xx} & 0 & 0 \\ \alpha'_{xy} & 0 & 0 & 0 & \mu_{yy} & 0 \\ 0 & 0 & 0 & 0 & 0 & \mu_{zz} \end{pmatrix} \quad (2.52)$$

$$\tilde{\Delta} = \begin{pmatrix} \alpha_{xy} & 0 & 0 & \mu_{yy} - \frac{N_0^2 \sin^2 \theta_0}{\varepsilon_{zz}} \\ 0 & \alpha_{xy} & -\mu_{xx} & 0 \\ 0 & \frac{N_0^2 \sin^2 \theta_0}{\mu_{zz}} - \varepsilon_{yy} & \alpha_{xy} & 0 \\ \varepsilon_{xx} & 0 & 0 & \alpha_{xy} \end{pmatrix} \quad (2.53)$$

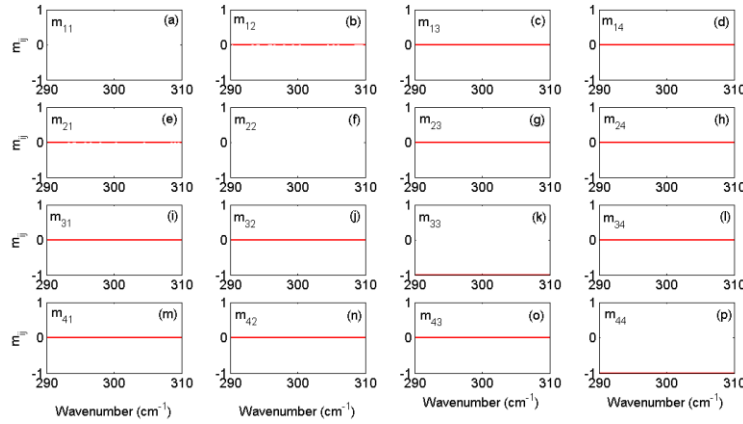


Figure 2.8 Normalized Mueller matrix components for $\begin{pmatrix} 0 & \alpha_{xy} & 0 \\ -\alpha_{xy} & 0 & 0 \\ 0 & 0 & 0 \end{pmatrix}$ ME tensor symmetry. Model contains one oscillator with $S_{\alpha,xy} = 0.01$; $\omega_0 = 300 \text{ cm}^{-1}$; $\gamma = 2$; dielectric constant $\varepsilon_{xx} = \varepsilon_{yy} = \varepsilon_{zz} = 10$; magnetic permeability $\mu_{xx} = \mu_{yy} = \mu_{zz} = 1$; $AOI = 60^\circ$

$$M = \begin{pmatrix} \epsilon_{xx} & 0 & 0 & 0 & 0 & 0 \\ 0 & \epsilon_{yy} & 0 & 0 & 0 & \alpha_{yz} \\ 0 & 0 & \epsilon_{zz} & 0 & -\alpha_{yz} & 0 \\ 0 & 0 & 0 & \mu_{xx} & 0 & 0 \\ 0 & 0 & -\alpha_{yz}^* & 0 & \mu_{yy} & 0 \\ 0 & \alpha_{yz}^* & 0 & 0 & 0 & \mu_{zz} \end{pmatrix} \quad (2.54)$$

$$\tilde{\Delta} = \begin{pmatrix} 0 & -\alpha_{yz} & 0 & \mu_{yy} + \frac{N_0 \sin \theta_0 (\alpha_{yz} - N_0 \sin \theta_0)}{\epsilon_{zz}} \\ 0 & 0 & -\mu_{xx} & 0 \\ \frac{\alpha_{yz} (\alpha_{yz} - N_0 \sin \theta_0)}{\mu_{zz}} & -\epsilon_{yy} - \frac{N_0 \sin \theta_0 (\alpha_{yz} - N_0 \sin \theta_0)}{\mu_{zz}} & 0 & 0 \\ \epsilon_{xx} & 0 & 0 & 0 \end{pmatrix} \quad (2.55)$$

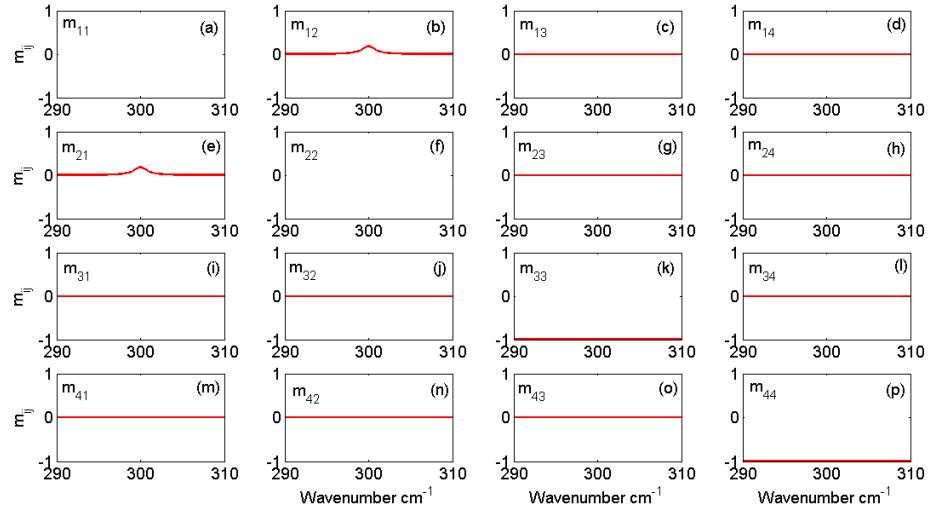


Figure 2.9 Normalized Mueller matrix components for $\begin{pmatrix} 0 & 0 & 0 \\ 0 & 0 & \alpha_{yz} \\ 0 & -\alpha_{yz} & 0 \end{pmatrix}$ ME tensor symmetry. Model contains one oscillator with $S_{\alpha,yz} = 0.01$; $\omega_0 = 300 \text{ cm}^{-1}$, $\gamma = 2$; dielectric constant $\epsilon_{xx} = \epsilon_{yy} = \epsilon_{zz} = 10$; magnetic permeability $\mu_{xx} = \mu_{yy} = \mu_{zz} = 1$; $AOI = 60^\circ$.

$$M = \begin{pmatrix} \varepsilon_{xx} & 0 & 0 & 0 & 0 & \alpha_{xz} \\ 0 & \varepsilon_{yy} & 0 & 0 & 0 & 0 \\ 0 & 0 & \varepsilon_{zz} & -\alpha_{xz} & 0 & 0 \\ 0 & 0 & -\alpha_{xz}^* & \mu_{xx} & 0 & 0 \\ 0 & 0 & 0 & 0 & \mu_{yy} & 0 \\ \alpha_{xz}^* & 0 & 0 & 0 & 0 & \mu_{zz} \end{pmatrix} \quad (2.56)$$

$$\tilde{\Delta} = \begin{pmatrix} 0 & 0 & \frac{\alpha_{xz} N_0 \sin \theta_0}{\varepsilon_{zz}} & \mu_{yy} - \frac{N_0^2 \sin^2 \theta_0}{\varepsilon_{zz}} \\ 0 & 0 & \frac{\alpha_{xz}^2}{\varepsilon_{zz}} - \mu_{xx} & \frac{\alpha_{xz} N_0 \sin \theta_0}{\varepsilon_{zz}} \\ -\frac{\alpha_{xz} N_0 \sin \theta_0}{\mu_{zz}} & \frac{N_0^2 \sin^2 \theta_0}{\mu_{zz}} - \varepsilon_{yy} & 0 & 0 \\ -\frac{\alpha_{xz}^2}{\mu_{zz}} + \varepsilon_{xx} & \frac{\alpha_{xz} N_0 \sin \theta_0}{\mu_{zz}} & 0 & 0 \end{pmatrix} \quad (2.57)$$

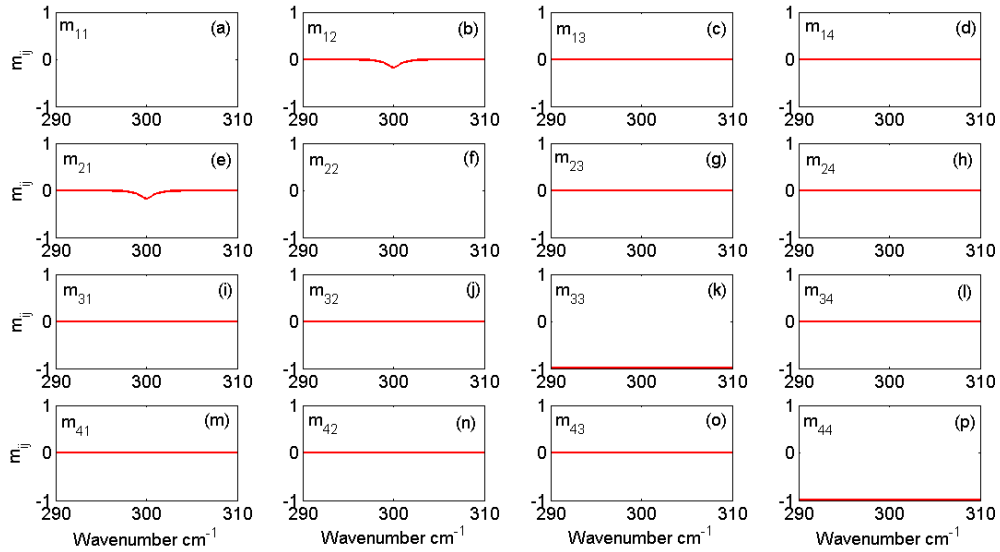


Figure 2.10 Normalized Mueller matrix components for $\begin{pmatrix} 0 & 0 & \alpha_{xz} \\ 0 & 0 & 0 \\ -\alpha_{xz} & 0 & 0 \end{pmatrix}$ ME tensor

symmetry. Model contains one oscillator with $S_{\alpha,xz} = 0.01$; $\omega_0 = 300 \text{ cm}^{-1}$, $\gamma = 2$; dielectric constant $\varepsilon_{xx} = \varepsilon_{yy} = \varepsilon_{zz} = 10$; magnetic permeability $\mu_{xx} = \mu_{yy} = \mu_{zz} = 1$; $AOI = 60^\circ$.

$$M = \begin{pmatrix} \epsilon_{xx} & 0 & 0 & \alpha_{xx} & 0 & 0 \\ 0 & \epsilon_{yy} & 0 & 0 & 0 & 0 \\ 0 & 0 & \epsilon_{zz} & 0 & 0 & 0 \\ \alpha_{xx}^* & 0 & 0 & \mu_{xx} & 0 & 0 \\ 0 & 0 & 0 & 0 & \mu_{yy} & 0 \\ 0 & 0 & 0 & 0 & 0 & \mu_{zz} \end{pmatrix} \quad (2.58)$$

$$\tilde{\Delta} = \begin{pmatrix} 0 & 0 & 0 & \mu_{yy} - \frac{N_0^2 \sin^2 \theta_0}{\epsilon_{zz}} \\ -\alpha_{xx} & 0 & -\mu_{xx} & 0 \\ 0 & \frac{N_0^2 \sin^2 \theta_0}{\mu_{zz}} - \epsilon_{yy} & 0 & 0 \\ \epsilon_{xx} & 0 & \alpha_{xx} & 0 \end{pmatrix} \quad (2.59)$$

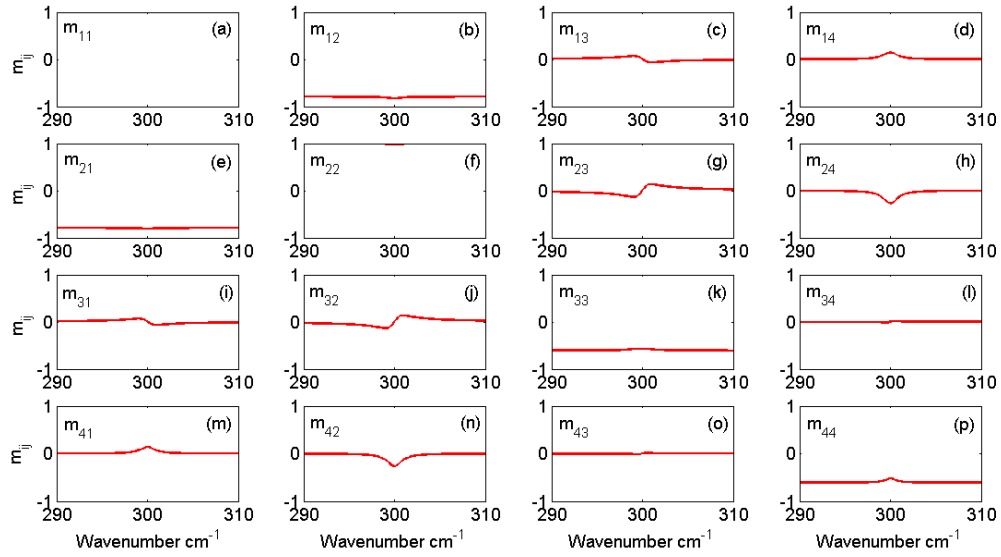


Figure 2.11 Normalized Mueller matrix components for $\begin{pmatrix} \alpha_{xx} & 0 & 0 \\ 0 & 0 & 0 \\ 0 & 0 & 0 \end{pmatrix}$ ME tensor

symmetry. Model contains one oscillator with $S_{\alpha,xx} = 0.01$; $\omega_0 = 300 \text{ cm}^{-1}$, $\gamma = 2$; dielectric constant $\epsilon_{xx} = \epsilon_{yy} = \epsilon_{zz} = 10$; magnetic permeability $\mu_{xx} = \mu_{yy} = \mu_{zz} = 1$; $AOI = 60^\circ$.

$$M = \begin{pmatrix} \varepsilon_{xx} & 0 & 0 & 0 & 0 & 0 \\ 0 & \varepsilon_{yy} & 0 & 0 & \alpha_{yy} & 0 \\ 0 & 0 & \varepsilon_{zz} & 0 & 0 & 0 \\ 0 & 0 & 0 & \mu_{xx} & 0 & 0 \\ 0 & \alpha_{yy}^* & 0 & 0 & \mu_{yy} & 0 \\ 0 & 0 & 0 & 0 & 0 & \mu_{zz} \end{pmatrix} \quad (2.60)$$

$$\tilde{\Delta} = \begin{pmatrix} 0 & \alpha_{yy} & 0 & \mu_{yy} - \frac{N_0^2 \sin^2 \theta_0}{\varepsilon_{zz}} \\ 0 & 0 & -\mu_{xx} & 0 \\ 0 & \frac{N_0^2 \sin^2 \theta_0}{\mu_{zz}} - \varepsilon_{yy} & 0 & -\alpha_{yy} \\ \varepsilon_{xx} & 0 & 0 & 0 \end{pmatrix} \quad (2.61)$$

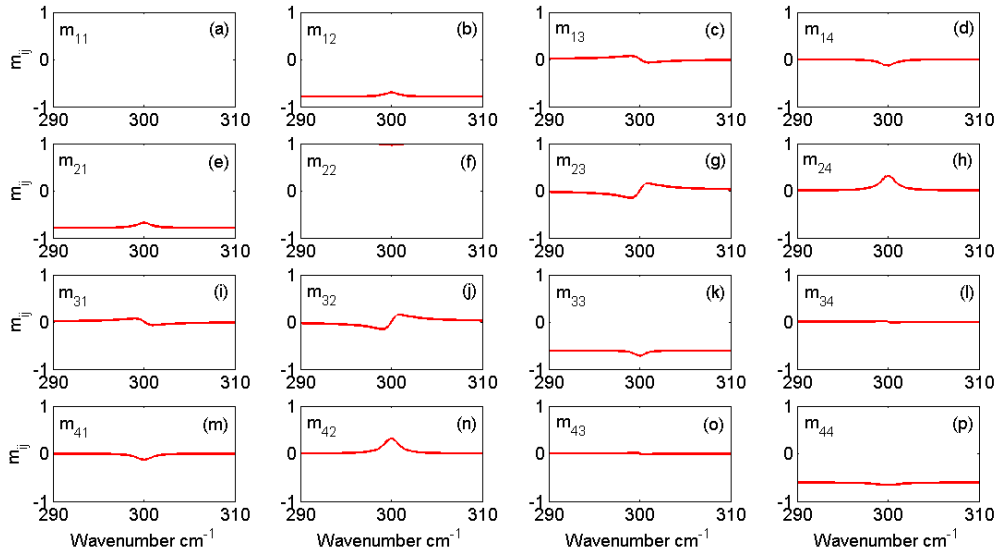


Figure 2.12 Normalized Mueller matrix components for $\begin{pmatrix} 0 & 0 & 0 \\ 0 & \alpha_{yy} & 0 \\ 0 & 0 & 0 \end{pmatrix}$ ME tensor

symmetry. Model contains one oscillator with $S_{\alpha,yy} = 0.01$; $\omega_0 = 300 \text{ cm}^{-1}$, $\gamma = 2$; dielectric constant $\varepsilon_{xx} = \varepsilon_{yy} = \varepsilon_{zz} = 10$; magnetic permeability $\mu_{xx} = \mu_{yy} = \mu_{zz} = 1$; $AOI = 60^\circ$.

$$M = \begin{pmatrix} \epsilon_{xx} & 0 & 0 & 0 & 0 & 0 \\ 0 & \epsilon_{yy} & 0 & 0 & 0 & 0 \\ 0 & 0 & \epsilon_{zz} & 0 & 0 & \alpha_{zz} \\ 0 & 0 & 0 & \mu_{xx} & 0 & 0 \\ 0 & 0 & 0 & 0 & \mu_{yy} & 0 \\ 0 & 0 & \alpha_{zz}^* & 0 & 0 & \mu_{zz} \end{pmatrix} \quad (2.62)$$

$$\tilde{\Delta} = \begin{pmatrix} 0 & -\frac{N_0^2 \sin^2 \theta_0 \alpha_{zz}}{\epsilon_{zz} \mu_{zz} - \alpha_{zz}^2} & 0 & \mu_{yy} - \frac{N_0^2 \sin^2 \theta_0 \mu_{zz}}{\epsilon_{zz} \mu_{zz} - \alpha_{zz}^2} \\ 0 & 0 & -\mu_{xx} & 0 \\ 0 & \frac{N_0^2 \sin^2 \theta_0 \epsilon_{zz}}{\epsilon_{zz} \mu_{zz} - \alpha_{zz}^2} - \epsilon_{yy} & 0 & \frac{N_0^2 \sin^2 \theta_0 \alpha_{zz}}{\epsilon_{zz} \mu_{zz} - \alpha_{zz}^2} \\ \epsilon_{xx} & 0 & 0 & 0 \end{pmatrix} \quad (2.63)$$

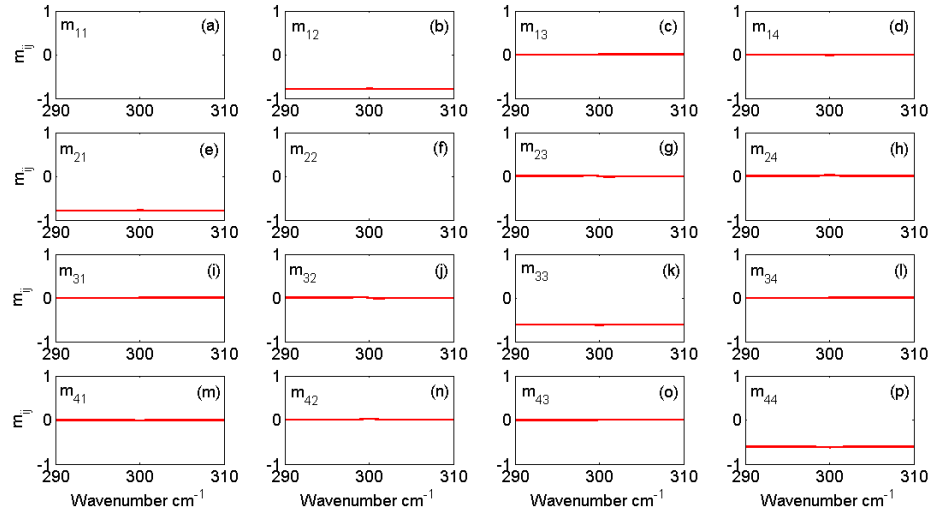


Figure 2.13 Normalized Mueller matrix components for $\begin{pmatrix} 0 & 0 & 0 \\ 0 & 0 & 0 \\ 0 & 0 & \alpha_{zz} \end{pmatrix}$ ME tensor

symmetry. Model contains one oscillator with $S_{\alpha,zz} = 0.01$; $\omega_0 = 300 \text{ cm}^{-1}$, $\gamma = 2$; dielectric constant $\epsilon_{xx} = \epsilon_{yy} = \epsilon_{zz} = 10$; magnetic permeability $\mu_{xx} = \mu_{yy} = \mu_{zz} = 1$; $AOI = 60^\circ$.

Table 2.2 Dependence of the MM components on the symmetry-allowed ME interaction. The ME tensor components are in the left column, MM spectra are in the middle column, and the comments are in the right column.

ME tensor	MM plot	α appearance in MM components
$\begin{pmatrix} 0 & \alpha_{xy} & 0 \\ \alpha_{xy}^* & 0 & 0 \\ 0 & 0 & 0 \end{pmatrix}$		None
$\begin{pmatrix} 0 & 0 & 0 \\ 0 & 0 & \alpha_{yz} \\ 0 & \alpha_{yz}^* & 0 \end{pmatrix}$		m_{12}, m_{21}
$\begin{pmatrix} 0 & 0 & \alpha_{xz} \\ 0 & 0 & 0 \\ \alpha_{xz}^* & 0 & 0 \end{pmatrix}$		m_{12}, m_{21}
$\begin{pmatrix} \alpha_{xx} & 0 & 0 \\ 0 & 0 & 0 \\ 0 & 0 & 0 \end{pmatrix}$		Diagonal weak Off-diagonal strong
$\begin{pmatrix} 0 & 0 & 0 \\ 0 & \alpha_{yy} & 0 \\ 0 & 0 & 0 \end{pmatrix}$		Diagonal weak Off-diagonal strong
$\begin{pmatrix} 0 & 0 & 0 \\ 0 & 0 & 0 \\ 0 & 0 & \alpha_{zz} \end{pmatrix}$		All weak

It should be noted as well that the strength of magneto-electric features in Mueller matrix spectra components depends on the background values of ε and μ . We pointed out earlier that magneto-electric interaction is bounded by the geometric mean of the diagonalized permittivity and permeability tensors. The closer α approaches to this thermodynamic limit the stronger contribution in MM components. Simultaneous increase in values of ε , μ and α , when Equation (1.3) still holds, results in more stronger appearance in MM components of ME contribution.

The main result of simulations presented in Table 2.2 is a demonstration of the fact that MM spectroscopic ellipsometry that measures all spectral components presented in Figures 2.8 – 2.13 can distinguish different symmetries of the α tensor. For example, α_{xx} and α_{yy} peaks have different sign (positive and negative) in the spectra of m_{23} and m_{24} .

CHAPTER 3

ELECTROMAGNETIC WAVE PROPAGATION IN BI-ANISOTROPIC MULTILAYER STRUCTURES

In this Chapter original results are shown for calculation techniques for the wave propagation in bi-anisotropic multilayer systems. As shown in the previous Chapter, methods for wave propagation in bulk materials were based on the matrices L_{in} and L_{out} in the form of Equation (2.22) and Equation (2.29). For general anisotropic media when transmitted modes are coupled, Equation (2.29) should be used to find the L_{out} matrix. In order to take into account the optical response from thin film layers sandwiched between ambient and substrate one should construct matrices which project xy -components of the fields through all layers, from the top interface to the bottom interface. There are two common strategies of obtaining these matrices. In the first case, which is more detailed but not so desirable for obtaining analytical solutions, we will refer to as a “layer matrix L ” method. This approach requires calculations of eigenvectors of each layer’s $\tilde{\Delta}$ matrix

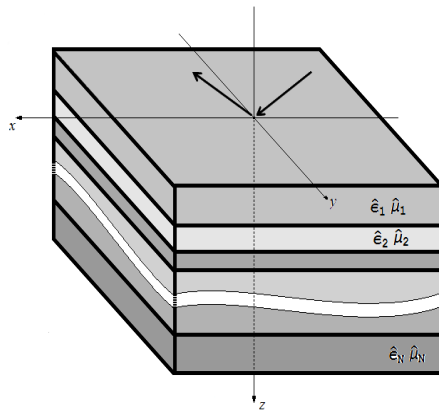


Figure 3.1 General schematics for a bi-anisotropic multilayer system. Incident wave is in the xz -plane. Positive z -direction is vertically down.

and, based on a trivial solution of the matrix wave equation, constructing propagating matrix K . Second method uses Cayley-Hamilton theorem [13] from linear algebra which provides a faster way to obtaining layer matrix without calculating eigenvectors. We will call layer matrix partial transfer matrix T_p in this case. For discussion of advantages and disadvantages of each method we solve in the beginning anisotropic double layer system without ME activity problem on isotropic substrate, show consistency with previous developed works and then give general analytical expressions of Fresnel's coefficients for arbitrary systems (Figure 3.1) using second method. We also show simulation of optical response for a single layer, bilayer and a superlattice structure with N bilayers for some cases of certain ME tensor symmetry in terms of MM and reflectance and compare it with numerical calculations. In the final section we briefly discuss simulating/fitting software developed as a part of this Thesis. Graphical user interface will be presented and some capabilities explained.

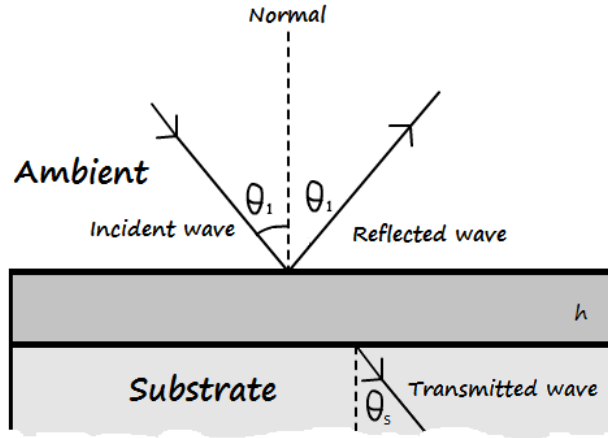


Figure 3.2 Scheme for anisotropic single thin film wave propagation.

3.1 Prior Works for Thin Films

Light propagation in thin films has been studied in a number of theoretical papers. The review can be found in P.Rogers *et al* [9]. Here we present the summary for the most important theoretical developments for single layer systems on isotropic substrate from P. Rogers' Theses and his papers [9,10]. Sketch of the system and wave propagation is shown in Figure 3.2. Fresnel's coefficients solutions are shown below.

$$\begin{aligned}
 r_{pp} &= \frac{q_{zp} \cos(q_{zp}h) \left(\frac{N_s}{N_0} k_{z0} - \frac{N_0}{N_2} k_{zs} \right) + i \left(\frac{N_0 N_2 q_{zp}^2}{\epsilon_{xx}} - \frac{\epsilon_{xx} k_{z0} k_{zs}}{N_0 N_2} \right) \sin(q_{zp}h)}{q_{zp} \cos(q_{zp}h) \left(\frac{N_s}{N_0} k_{z0} + \frac{N_0}{N_2} k_{zs} \right) - i \left(\frac{N_0 N_2 q_{zp}^2}{\epsilon_{xx}} + \frac{\epsilon_{xx} k_{z0} k_{zs}}{N_0 N_2} \right) \sin(q_{zp}h)}; r_{ss} = \frac{q_{zs} \cos(q_{zs}h) (k_{z0} - k_{zs}) + i \left(\frac{q_{zp}^2}{\mu_{xx}} - k_{z0} k_{zs} \mu_{xx} \right) \sin(q_{zs}h)}{q_{zs} \cos(q_{zs}h) (k_{z0} + k_{zs}) - i \left(\frac{q_{zp}^2}{\mu_{xx}} + k_{z0} k_{zs} \mu_{xx} \right) \sin(q_{zs}h)} \\
 t_{pp} &= \frac{2k_{z0} q_{zp}}{q_{zp} \cos(q_{zp}h) \left(\frac{N_s}{N_0} k_{z0} + \frac{N_0}{N_2} k_{zs} \right) - i \left(\frac{N_0 N_2 q_{zp}^2}{\epsilon_{xx}} + \frac{\epsilon_{xx} k_{z0} k_{zs}}{N_0 N_2} \right) \sin(q_{zp}h)}; t_{ss} = \frac{2k_{z0} q_{zs}}{q_{zs} \cos(q_{zs}h) (k_{z0} + k_{zs}) - i \left(\frac{q_{zp}^2}{\mu_{xx}} + k_{z0} k_{zs} \mu_{xx} \right) \sin(q_{zs}h)}
 \end{aligned} \tag{3.1}$$

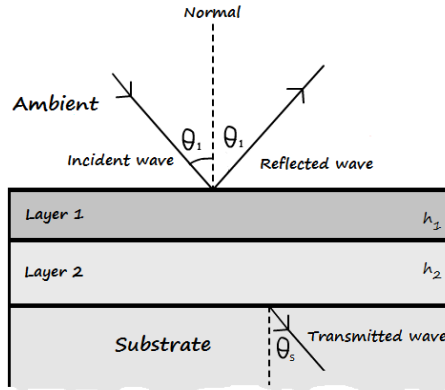


Figure 3.3 Scheme for anisotropic bilayer thin film wave propagation

3.2 Layer Matrix Technique and Analytical Solutions for Bilayer Anisotropic

Structure with Zero ME Tensor on Isotropic Substrate.

In this section our original results for bilayer structures are presented. In short, we have increased the number of anisotropic layers compared (Figure 3.3) to that has been done previously by P.Rogers [9]. This step is conceptually important since it leads to the future

development of the theory for multilayers and superlattices. The latter could be considered as 1D metamaterials, thus bringing together several directions of our research. We use layer matrix technique in this case.

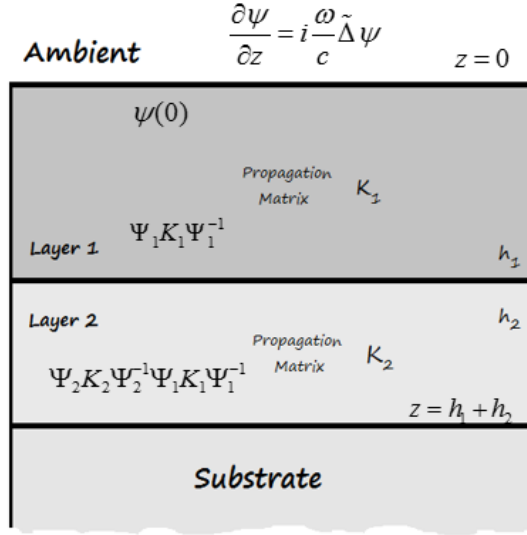


Figure 3.4. Notations for a bilayer structure calculations using a layer matrix L method.

In the chapter on bulk structures we got explicit expression for matrix wave Equation (2.13). When $\tilde{\Delta}$ matrix does not depends on z we can integrate it and obtain

$$\psi(z) = e^{i \frac{\omega}{c} \tilde{\Delta} z} \psi(0) \quad (3.2)$$

For each particular mode solution becomes:

$$\psi_i(z) = e^{i \frac{\omega}{c} q_{z,i} z} \psi_i(0) \quad (3.3)$$

Let's consider detail structure of the electromagnetic wave inside the multilayers (Figure 3.4). Each mode variation inside a layer is shown in Equation (3.3). Thus if we want to construct a matrix, which contains all optical modes, such a matrix, which relates modes

at the interfaces of the n and $n-1$ layers, must have the form shown below. It is called a propagation matrix K .

$$\Psi_i = \begin{pmatrix} \psi_1^{(N)} & \psi_2^{(N)} & \psi_3^{(N)} & \psi_4^{(N)} \end{pmatrix} \quad (3.4)$$

$$K_i = \begin{pmatrix} e^{iq_{11}^{(N)}h} & 0 & 0 & 0 \\ 0 & e^{iq_{22}^{(N)}h} & 0 & 0 \\ 0 & 0 & e^{iq_{33}^{(N)}h} & 0 \\ 0 & 0 & 0 & e^{iq_{44}^{(N)}h} \end{pmatrix} \quad (3.5)$$

In order to obtain layer matrix which relates all components at one interface to another one we write down:

$$L_i \Psi_i = \Psi_i K_i \quad (3.6)$$

It is easy to see that layer matrix can be expressed as

$$L_i = \Psi_i K_i \Psi_i^{-1} \quad (3.7)$$

If we have a multilayer structure, one needs to project components from n to $n+m$ layer by doing simple multiplication between each layer matrices $L_n L_{n+1} \dots L_{n+m}$. The resultant matrix, which project components from ambient interface to substrate interface, looks as follows

$$L = \prod_{i=1}^n L_i = \prod_{i=1}^n \Psi_i K_i \Psi_i^{-1} \quad (3.8)$$

The layer matrix for a bilayer structure can be obtained as shown below. In the previous Chapter on bulk structures in Equation (2.23) we showed boundary conditions for an ambient-substrate interface.

$$L = L_1 L_2 = \Psi_2 K_2 \Psi_2^{-1} \Psi_1 K_1 \Psi_1^{-1} = \begin{pmatrix} l_{11} & l_{12} & l_{13} & l_{14} \\ l_{21} & l_{22} & l_{23} & l_{24} \\ l_{31} & l_{32} & l_{33} & l_{34} \\ l_{41} & l_{42} & l_{43} & l_{44} \end{pmatrix} \quad (3.9)$$

After adding layer matrix and modifying Equation (2.23) for bilayer structure with isotropic substrate we obtain:

$$\begin{pmatrix} E_{tp} \cos \theta_s \\ N_s E_{tp} \\ E_{ts} \\ N_s E_{ts} \cos \theta_s \end{pmatrix} = \begin{pmatrix} l_{11} & l_{12} & l_{13} & l_{14} \\ l_{21} & l_{22} & l_{23} & l_{24} \\ l_{31} & l_{32} & l_{33} & l_{34} \\ l_{41} & l_{42} & l_{43} & l_{44} \end{pmatrix} \begin{pmatrix} (E_{ip} - E_{rp}) \cos \theta_0 \\ N_0 (E_{ip} + E_{rp}) \\ E_{is} + E_{rs} \\ N_0 (E_{is} - E_{rs}) \cos \theta_0 \end{pmatrix} \quad (3.10)$$

The system ratios $\frac{E_{rp}}{E_{ip}}, \frac{E_{tp}}{E_{ip}}, \frac{E_{rs}}{E_{is}}, \frac{E_{ts}}{E_{is}}$ can be easily found, which give reflection and

transmission coefficients for media, or more explicitly:

$$r = \begin{pmatrix} r_{pp} & r_{ps} \\ r_{sp} & r_{ss} \end{pmatrix} = \frac{1}{a_{rs} b_{rp} - a_{rp} b_{rs}} \begin{pmatrix} a_{ip} b_{rs} - a_{rs} b_{ip} & a_{is} b_{rs} - a_{rs} b_{is} \\ a_{rp} b_{ip} - a_{ip} b_{rp} & a_{rp} b_{is} - a_{is} b_{rp} \end{pmatrix} \quad (3.11)$$

with $a_{ip}, a_{rp}, a_{is}, a_{rs}, b_{ip}, b_{rp}, b_{is}, b_{rs}$ are given by

$$\begin{aligned} a_{ip} &= \cos \theta_0 (l_{11} N_2 - l_{21} \cos \theta_2) + N_0 (l_{12} N_2 - l_{22} \cos \theta_2) \\ a_{rp} &= -\cos \theta_0 (l_{11} N_2 - l_{21} \cos \theta_2) + N_0 (l_{12} N_2 - l_{22} \cos \theta_2) \\ a_{is} &= N_0 \cos \theta_0 (l_{14} N_2 - l_{24} \cos \theta_2) + (l_{13} N_2 - l_{23} \cos \theta_2) \\ a_{rs} &= -N_0 \cos \theta_0 (l_{14} N_2 - l_{24} \cos \theta_2) + (l_{13} N_2 - l_{23} \cos \theta_2) \\ b_{ip} &= \cos \theta_0 (l_{31} N_2 \cos \theta_2 - l_{41}) + N_0 (l_{32} N_2 \cos \theta_2 - l_{42}) \\ b_{rp} &= -\cos(\theta_0) (l_{31} N_2 \cos(\theta_2) - l_{41}) + N_0 (l_{32} N_2 \cos(\theta_2) - l_{42}) \\ b_{is} &= N_0 \cos(\theta_0) (l_{34} N_2 \cos(\theta_2) - l_{44}) + (l_{33} N_2 \cos(\theta_2) - l_{43}) \\ b_{rs} &= -N_0 \cos(\theta_0) (l_{34} N_2 \cos(\theta_2) - l_{44}) + (l_{33} N_2 \cos(\theta_2) - l_{43}) \end{aligned} \quad (3.12)$$

Fresnel's coefficients for transmission can be found the same way, which gives

$$t = \begin{pmatrix} t_{pp} & t_{ps} \\ t_{sp} & t_{ss} \end{pmatrix} \quad (3.13)$$

$$\begin{aligned}
t_{pp} &= \frac{1}{N_2} (l_{21} \cos \theta_0 + l_{22} N_0 + r_{pp} (-l_{21} \cos \theta_0 + l_{22} N_0) + r_{sp} (l_{23} - l_{24} N_0 \cos \theta_0)) \\
t_{ps} &= \frac{1}{N_2} (l_{23} + l_{24} N_0 \cos \theta_0 + r_{ps} (-l_{21} \cos \theta_0 + l_{22} N_0) + r_{ss} (l_{23} - l_{24} N_0 \cos \theta_0)) \\
t_{sp} &= l_{31} \cos \theta_0 + l_{32} N_0 + r_{pp} (-l_{31} \cos \theta_0 + l_{32} N_0) + r_{sp} (l_{33} - l_{34} N_0 \cos \theta_0) \\
t_{ss} &= l_{33} + l_{34} N_0 \cos \theta_0 + r_{ps} (-l_{31} \cos \theta_0 + l_{32} N_0) + r_{ss} (l_{33} - l_{34} N_0 \cos \theta_0)
\end{aligned} \tag{3.14}$$

Finally we can obtain analytical expressions for Fresnel's coefficients:

$$\begin{aligned}
t_{pp} &= \frac{-4e^{ih_q q_{p1}} k_{z0} N_0 N_2 q_{zp1} q_{zp2} \varepsilon_{xx1} \varepsilon_{xx2}}{e^{2ih_q q_{p1}} \bar{N}_{p,0-} (q_{zp2} \bar{N}_{p,2-} \varepsilon_{xx2} \cos(h_2 q_{zp2}) + i \bar{N}_{p-} \sin(h_2 q_{zp2})) + \bar{N}_{p,0+} (-q_{zp2} \bar{N}_{p,2+} \varepsilon_{xx2} \cos(h_2 q_{zp2}) + i \bar{N}_{p+} \sin(h_2 q_{zp2}))} \\
t_{ss} &= \frac{-4e^{ih_q q_{s1}} k_{z0} q_{zs1} q_{zs2} \mu_{xx1} \mu_{xx2}}{e^{2ih_q q_{s1}} \bar{N}_{s,0-} (q_{zs2} \bar{N}_{s,2-} \mu_{xx2} \cos(h_2 q_{zs2}) + i \bar{N}_{s-} \sin(h_2 q_{zs2})) + \bar{N}_{s,0+} (-q_{zs2} \bar{N}_{s,2+} \mu_{xx2} \cos(h_2 q_{zs2}) + i \bar{N}_{s+} \sin(h_2 q_{zs2}))} \\
r_{pp} &= \frac{e^{2ih_q q_{p1}} \bar{N}_{p,0+} (-iq_{zp2} \bar{N}_{p,2-} \varepsilon_{xx2} \cos(h_2 q_{zp2}) + \bar{N}_{p-} \sin(h_2 q_{zp2})) + \bar{N}_{p,0-} (iq_{zp2} \bar{N}_{p,2+} \varepsilon_{xx2} \cos(h_2 q_{zp2}) + \bar{N}_{p+} \sin(h_2 q_{zp2}))}{e^{2ih_q q_{p1}} \bar{N}_{p,0-} (iq_{zp2} \bar{N}_{p,2-} \varepsilon_{xx2} \cos(h_2 q_{zp2}) - \bar{N}_{p-} \sin(h_2 q_{zp2})) + \bar{N}_{p,0+} (-iq_{zp2} \bar{N}_{p,2+} \varepsilon_{xx2} \cos(h_2 q_{zp2}) - \bar{N}_{p+} \sin(h_2 q_{zp2}))} \\
r_{ss} &= \frac{e^{2ih_q q_{s1}} \bar{N}_{s,0+} (iq_{zs2} \bar{N}_{s,2-} \mu_{xx2} \cos(h_2 q_{zs2}) + \bar{N}_{s-} \sin(h_2 q_{zs2})) + \bar{N}_{s,0-} (-iq_{zs2} \bar{N}_{s,2+} \mu_{xx2} \cos(h_2 q_{zs2}) - \bar{N}_{s+} \sin(h_2 q_{zs2}))}{e^{2ih_q q_{s1}} \bar{N}_{s,0-} (-iq_{zs2} \bar{N}_{s,2-} \mu_{xx2} \cos(h_2 q_{zs2}) + \bar{N}_{s-} \sin(h_2 q_{zs2})) + \bar{N}_{s,0+} (iq_{zs2} \bar{N}_{s,2+} \mu_{xx2} \cos(h_2 q_{zs2}) - \bar{N}_{s+} \sin(h_2 q_{zs2}))}
\end{aligned} \tag{3.15}$$

With coefficients

$$\begin{aligned}
\bar{N}_{p,0\pm} &= N_0^2 q_{zp1} \pm k_{z0} \varepsilon_{xx1} \\
\bar{N}_{p,2\pm} &= N_2^2 q_{zp1} \pm k_{z2} \varepsilon_{xx1} \\
\bar{N}_{p\pm} &= N_2^2 q_{zp2}^2 \varepsilon_{xx1} \pm k_{z2} q_{zp1} \varepsilon_{xx2}^2 \\
\bar{N}_{s,0\pm} &= q_{zs1} \pm k_{z0} \mu_{xx1} \\
\bar{N}_{s,2\pm} &= q_{zs1} \pm k_{z2} \mu_{xx1} \\
\bar{N}_{s\pm} &= q_{zs2}^2 \mu_{xx1} \pm k_{z2} q_{zs1} \mu_{xx2}^2
\end{aligned} \tag{3.16}$$

Next we show some optical response simulations obtained with the help of the derived formulas. Parameters for simulation are given in the table below.

Table 3.1 Parameters of the Lorentz model for the optical properties of the bilayer structure. The layer thickness $h_1=10\ \mu\text{m}$ and $h_2=90\ \mu\text{m}$ is in cm.

AOI 60°	Layer 1 $h_1 = 0.001$		Layer 2 $h_2 = 0.009$	
	$\varepsilon_\infty = 15$	$\mu_\infty = 1$	$\varepsilon_\infty = 15$	$\mu_\infty = 1$
ω	el 100	m 50	el 75	m 130
γ	1.5	1.5	1.5	1.5
S_x	0.1	0.02	0	0.01
S_y	0.1	0.04	0.3	0.01
S_z	0.1	0.01	0.1	0.01

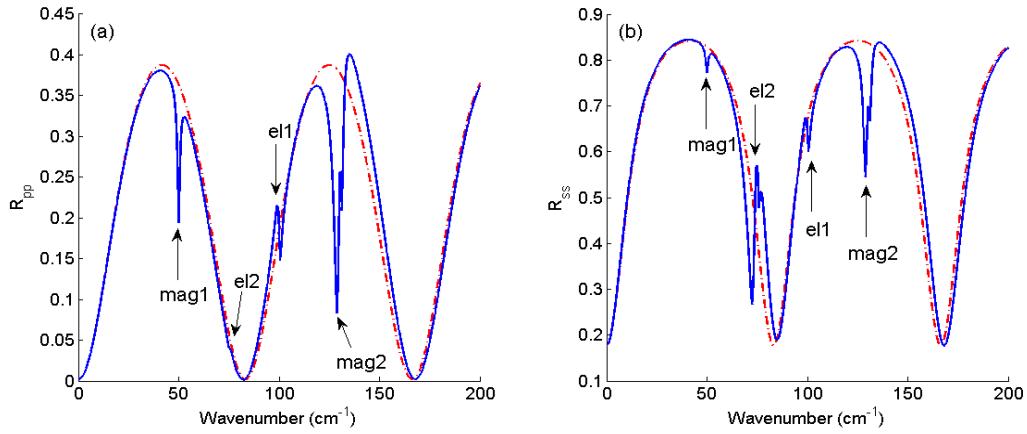


Figure 3.5 Simulation of (a) R_{pp} and (b) R_{ss} for bi-layer structure with anisotropic $\hat{\varepsilon}(\omega)$, $\hat{\mu}(\omega)$ and isotropic substrate. Red line is a reference calculation with zero oscillator strengths. Blue line is the calculated response with parameters from Table 3.1

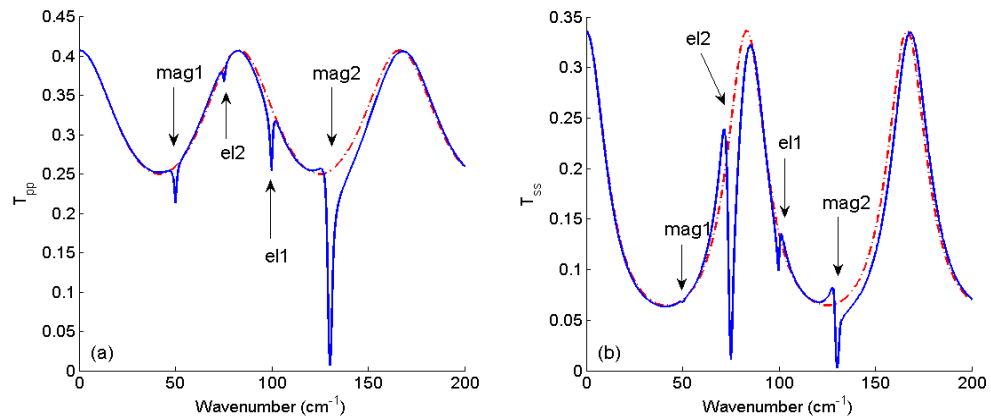


Figure 3.6 Simulation of (a) T_{pp} and (b) T_{ss} for bi-layer structure with anisotropic $\hat{\varepsilon}(\omega)$, $\hat{\mu}(\omega)$ and isotropic substrate. Red line is a reference calculation with zero oscillator strengths. Blue line is the calculated response with parameters from Table 3.1

3.3 Transfer Matrix Technique and Analytical Solutions for General Multilayer Bi-anisotropic structures.

In this section we use transfer matrix formalism for obtaining the most general form of solutions for arbitrary symmetry systems on anisotropic substrate. At the end of this Section we will compare the layer matrix and transfer matrix techniques.

Information about $\psi(z)$ knowing $\psi(0)$ is provided in Equation (3.2). In other words, we start from projections of incident and reflected light on ambient interface and moving through layers till we get to the last substrate interface. There is a more convenient way to obtain solutions. Let's assume that our final matrix equation should be in the form

$$\begin{pmatrix} E_{ts} \\ E_{rs} \\ E_{ip} \\ E_{rp} \end{pmatrix} = T \begin{pmatrix} E_{ts} \\ 0 \\ E_{ip} \\ 0 \end{pmatrix} = \begin{pmatrix} T_{11} & T_{12} & T_{13} & T_{14} \\ T_{21} & T_{22} & T_{23} & T_{24} \\ T_{31} & T_{32} & T_{33} & T_{34} \\ T_{41} & T_{42} & T_{43} & T_{44} \end{pmatrix} \begin{pmatrix} E_{ts} \\ 0 \\ E_{ip} \\ 0 \end{pmatrix} \quad (3.17)$$

where T is the so called transfer matrix, which will be constructed below. It is a better choice (no need to construct projection matrix from the xy -components at substrate interface to transmitted waves, which contains inverse eigenvectors components of the substrate's $\tilde{\Delta}$ matrix as in Equation (2.25) from the previous Chapter) to start from transmitted modes E_{ts} and E_{ip} , and move to the incident and reflected ones in ambient.

For this purpose we rewrite Equation (3.2) in the following form:

$$\psi(0) = e^{-i\frac{\omega}{c}\tilde{\Delta}z} \psi(z) \quad (3.18)$$

Now we can start from using $\psi(z)$ and move back to $\psi(0)$. In Equation (3.18) matrix exponent is nothing else but matrix which relates components at different interfaces. We call it a partial transfer matrix T_p . Instead of calculating layer matrix, which has a relatively complicated structure, we need to get an expression for matrix exponent, which is basically infinite series.

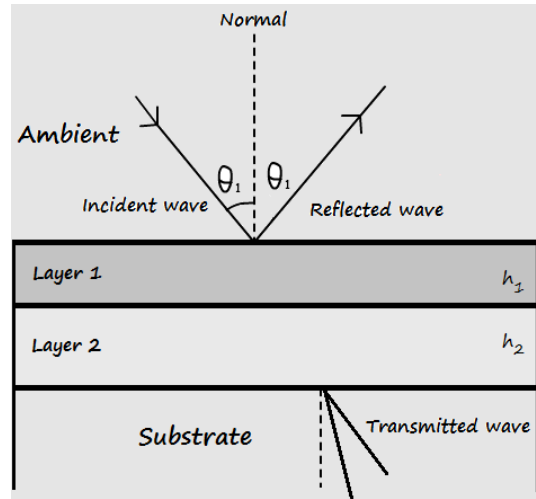


Figure 3.7 Ray propagation schematics in bilayer system.

In this situation the Cayley-Hamilton theorem is very useful. In short, the theorem states that every square matrix satisfies its own characteristic equation. Wohler *et al.* [13] applied this theorem to partial transfer matrix and showed that matrix exponent can be written as a polynomial of the order of $r-1$, where r is the rank of the matrix, with coefficients solely depended on eigenvalues. Analytical expression is the following:

$$T_p = e^{-i\frac{\omega}{c}\tilde{\Delta}z} = \beta_0 I + \beta_1 \tilde{\Delta} + \beta_2 \tilde{\Delta}^2 + \beta_3 \tilde{\Delta}^3 \quad (3.19)$$

with coefficients defined as

$$\begin{aligned}
\beta_0 &= -\sum_{j=1}^4 q_k q_l q_m \frac{e^{-i\frac{\omega}{c}q_j z}}{(q_j - q_k)(q_j - q_l)(q_j - q_m)} \\
\beta_1 &= \sum_{j=1}^4 (q_k q_l + q_k q_m + q_l q_m) \frac{e^{-i\frac{\omega}{c}q_j z}}{(q_j - q_k)(q_j - q_l)(q_j - q_m)} \\
\beta_2 &= -\sum_{j=1}^4 (q_k + q_l + q_m) \frac{e^{-i\frac{\omega}{c}q_j z}}{(q_j - q_k)(q_j - q_l)(q_j - q_m)} \\
\beta_3 &= \sum_{j=1}^4 \frac{e^{-i\frac{\omega}{c}q_j z}}{(q_j - q_k)(q_j - q_l)(q_j - q_m)}
\end{aligned} \tag{3.20}$$

and q_j are eigenvalues of $\tilde{\Delta}$ matrix. For obtaining expressions for eigenvalues the following equation should be solved

$$\begin{pmatrix} \Delta_{11} & \Delta_{12} & \Delta_{13} & \Delta_{14} \\ \Delta_{21} & \Delta_{22} & \Delta_{23} & \Delta_{24} \\ \Delta_{31} & \Delta_{32} & \Delta_{33} & \Delta_{34} \\ \Delta_{41} & \Delta_{42} & \Delta_{43} & \Delta_{44} \end{pmatrix} \begin{pmatrix} E_x \\ E_y \\ H_x \\ H_y \end{pmatrix} = q_z \begin{pmatrix} E_x \\ E_y \\ H_x \\ H_y \end{pmatrix} \tag{3.21}$$

as a result we get fourth order polynomial with complex coefficients. If we reduce high order coefficient we obtain the following equation:

$$q_z^4 + C_1 q_z^3 + C_2 q_z^2 + C_3 q_z + C_4 = 0 \tag{3.22}$$

“The Handbook of Functions” by Abramowits and Stegun [14] provides solutions of Equation (3.22). That means there are no difficulties to construct analytical expression for partial transfer matrix. If we have multilayer structure total propagating matrix is given as a product of partial transfer matrices of each layer $T_{p,1} \dots T_{p,i-1} T_{p,i}$. In the previous chapter we defined L_{in} in Equation (2.22) and L_{out} in Equation (2.50). In order to get solutions in the form of Equation (2.15) we can write:

$$\begin{pmatrix} E_{is} \\ E_{rs} \\ E_{ip} \\ E_{rp} \end{pmatrix} = T \begin{pmatrix} E_{ts} \\ 0 \\ E_{tp} \\ 0 \end{pmatrix} = L_{in} \prod_{i=1}^N T_{p,i} L_{out} \begin{pmatrix} E_{ts} \\ 0 \\ E_{tp} \\ 0 \end{pmatrix} = L_{in} \prod_{i=1}^N (\beta_{0i} I + \beta_{1i} \tilde{\Delta}_i + \beta_{2i} \tilde{\Delta}_i^2 + \beta_{3i} \tilde{\Delta}_i^3) L_{out} \begin{pmatrix} E_{ts} \\ 0 \\ E_{tp} \\ 0 \end{pmatrix} \quad (3.23)$$

After plugging in Equation (3.23) the expressions for L_{in} and L_{out} , we obtain the final form:

$$\begin{pmatrix} E_{is} \\ E_{rs} \\ E_{ip} \\ E_{rp} \end{pmatrix} = \frac{1}{2} \begin{pmatrix} 0 & 1 & -\frac{1}{N_0 \cos \theta_i} & 0 \\ 0 & 1 & \frac{1}{N_0 \cos \theta_i} & 0 \\ \frac{1}{\cos \theta_i} & 0 & 0 & \frac{1}{N_0} \\ -\frac{1}{\cos \theta_i} & 0 & 0 & \frac{1}{N_0} \end{pmatrix} \prod_{i=1}^N (\beta_{0i} I + \beta_{1i} \tilde{\Delta}_i + \beta_{2i} \tilde{\Delta}_i^2 + \beta_{3i} \tilde{\Delta}_i^3) \begin{pmatrix} \psi_{11}^{sub} & 0 & \psi_{12}^{sub} & 0 \\ \psi_{21}^{sub} & 0 & \psi_{22}^{sub} & 0 \\ \psi_{31}^{sub} & 0 & \psi_{32}^{sub} & 0 \\ \psi_{41}^{sub} & 0 & \psi_{42}^{sub} & 0 \end{pmatrix} \begin{pmatrix} E_{ts} \\ 0 \\ E_{tp} \\ 0 \end{pmatrix} \quad (3.24)$$

Transfer matrix is defined as

$$T = \frac{1}{2} \begin{pmatrix} 0 & 1 & -\frac{1}{N_0 \cos \theta_i} & 0 \\ 0 & 1 & \frac{1}{N_0 \cos \theta_i} & 0 \\ \frac{1}{\cos \theta_i} & 0 & 0 & \frac{1}{N_0} \\ -\frac{1}{\cos \theta_i} & 0 & 0 & \frac{1}{N_0} \end{pmatrix} \prod_{i=1}^N (\beta_{0i} I + \beta_{1i} \tilde{\Delta}_i + \beta_{2i} \tilde{\Delta}_i^2 + \beta_{3i} \tilde{\Delta}_i^3) \begin{pmatrix} \psi_{11}^{sub} & 0 & \psi_{12}^{sub} & 0 \\ \psi_{21}^{sub} & 0 & \psi_{22}^{sub} & 0 \\ \psi_{31}^{sub} & 0 & \psi_{32}^{sub} & 0 \\ \psi_{41}^{sub} & 0 & \psi_{42}^{sub} & 0 \end{pmatrix} \quad (3.25)$$

As we discuss earlier for biaxial substrates Equation (2.50) could be used, then

$$T = \frac{1}{2} \begin{pmatrix} 0 & 1 & -\frac{1}{N_0 \cos \theta_i} & 0 \\ 0 & 1 & \frac{1}{N_0 \cos \theta_i} & 0 \\ \frac{1}{\cos \theta_i} & 0 & 0 & \frac{1}{N_0} \\ -\frac{1}{\cos \theta_i} & 0 & 0 & \frac{1}{N_0} \end{pmatrix} \prod_{i=1}^N (\beta_{0i} I + \beta_{1i} \tilde{\Delta}_i + \beta_{2i} \tilde{\Delta}_i^2 + \beta_{3i} \tilde{\Delta}_i^3) \begin{pmatrix} 0 & 0 & \frac{q_{zp}}{\sqrt{q_x^2 + q_{zp}^2}} & 0 \\ 1 & 0 & 0 & 0 \\ \frac{q_{zs}}{\Delta_{23}} & 0 & 0 & 0 \\ 0 & 0 & \frac{1}{\Delta_{14}} \frac{q_{zp}^2}{\sqrt{q_x^2 + q_{zp}^2}} & 0 \end{pmatrix} \quad (3.26)$$

where right RHS matrix corresponds to substrate. Now it is easy to show solutions for Fresnel's coefficients:

$$\begin{aligned}
 r_{pp} &= \frac{T_{11}T_{43} - T_{13}T_{41}}{T_{11}T_{33} - T_{13}T_{31}} & t_{pp} &= \frac{T_{11}}{T_{11}T_{33} - T_{13}T_{31}} \\
 r_{sp} &= \frac{T_{11}T_{23} - T_{13}T_{21}}{T_{11}T_{33} - T_{13}T_{31}} & t_{sp} &= -\frac{T_{13}}{T_{11}T_{33} - T_{13}T_{31}} \\
 r_{ss} &= \frac{T_{21}T_{33} - T_{23}T_{31}}{T_{11}T_{33} - T_{13}T_{31}} & t_{ss} &= \frac{T_{33}}{T_{11}T_{33} - T_{13}T_{31}} \\
 r_{ps} &= \frac{T_{33}T_{41} - T_{31}T_{43}}{T_{11}T_{33} - T_{13}T_{31}} & t_{ps} &= -\frac{T_{31}}{T_{11}T_{33} - T_{13}T_{31}}
 \end{aligned} \tag{3.27}$$

To conclude, we compare layer matrix and transfer matrix techniques. When we use the layer matrix we start from ambient, project waves on the interface and then move through the layers by means of propagation matrix and arrive to the substrate. Then we project transmitted modes on the interface and finally obtain a solution. It was pointed out earlier that projecting transmitted modes on the interface involves matrix inverse operation which is not desirable for obtaining analytical solutions. Expression quickly becomes too bulky. The layer matrix gives some advantages though. We calculate eigenmodes for each layer and thus we know dynamics inside layers (Poynting vectors can be obtained fairly quickly). Energy conservation arguments are easier to justify knowing such information.

In the transfer matrix formalism we start from the substrate and represent substrate's fields projection in terms of transmitted waves (opposite to what we do using layer matrix L). Then we move from the last layer to ambient using partial transfer matrix. At the ambient interface we use L_{in} matrix to obtain p and s components of incident and reflected waves in terms of fields' projections. Then we get the solutions.

Partial transfer matrix does not contain any eigenmodes information and solely defined by the eigenvalues and by the elements of $\tilde{\Delta}$ matrix. We miss some information about waves propagation inside layers but get instead a faster method to obtain solutions and, as a result, more compact formulas. Both methods give the same results and both methods have their advantages and disadvantages.

Let's discuss the limitations for the applicability of our theoretical results, which cover only the linear optical effects and homogeneous layers without thickness gradient. We do not intend to cover the non-linear effects and inhomogeneous structures, which are outside of the scope of our work. For a non-linear media, certain approximations should be done to establish the relationship among the field vectors and to allow treating the material by means of the matrix formalism. For inhomogeneous media, the sample should be divided into regions where optical matrix does not depend on z , after that procedure described above can be applied for further analysis.

CHAPTER 4

MMFIT FITTING PROGRAM MANUAL

In this Chapter description of the developed MMFit program is given. There are three version of this software. One is for arbitrary bulk materials, second is for thin film layer on an anisotropic substrate, third is for a double layer superlattice on an anisotropic substrate. Both thin film layers and bulk layer can contain any combinations of electric, magnetic, magneto-electric and chiral oscillations. SHO model and Berreman formalism were utilized to get representation of pseudo-dielectric $\langle \epsilon \rangle$ function, ellipsometric Ψ, Δ , reflectance, transmittance and Mueller matrices. Maximum number of oscillators in this version is 36 which can be increased if needed. Levenberg-Marquardt algorithm was used for fitting, where number of iterations changing is available for user.

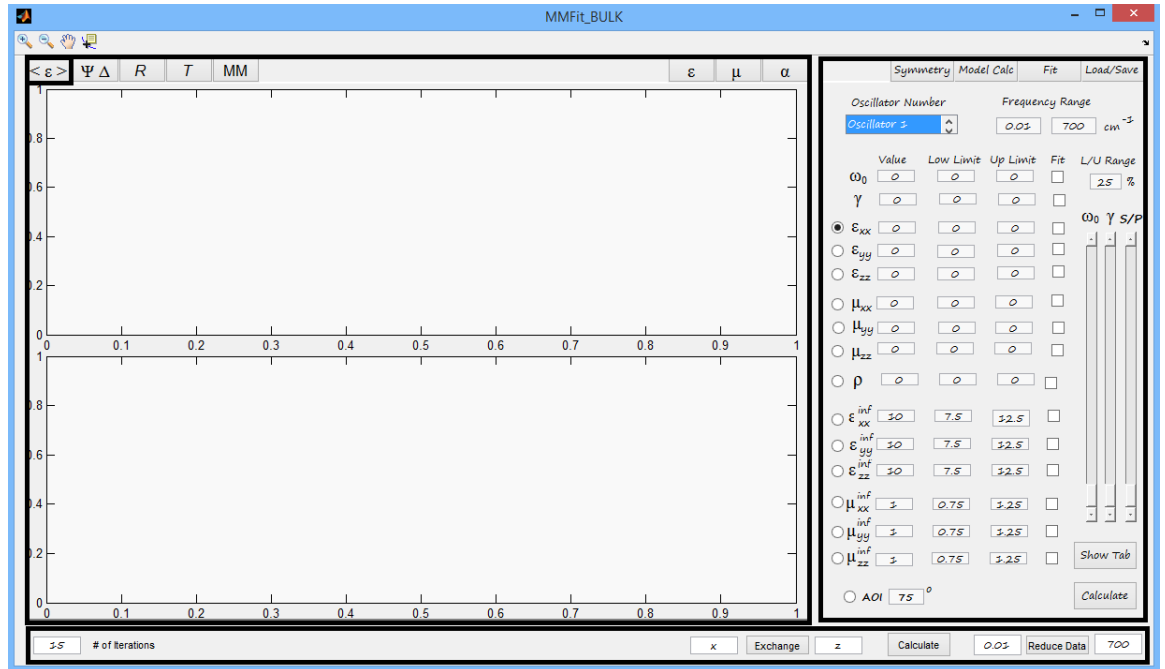


Figure 6.1 Start window of MMFit program. By default data panel (left) is for pseudo-dielectric function and model panel (right) is for model creation (“Model Calc”).

Program consists of three main panels. Left one, consisting of eight subpanels, is for data and models representation, right one, consisting from four to five subpanels in different versions, is for loading, saving data and models, adjusting fitting parameters, creation of models, choosing tensor symmetry. Low panel allows to adjust data (reduce to desirable range), choose number of iterations for fitting, calculate current model and exchange columns in current model (analog to Euler rotation by 90 degrees in any direction).

4.1 Working with Data

In order to load or save data and models one should click on “Load/Save” button in right panel.

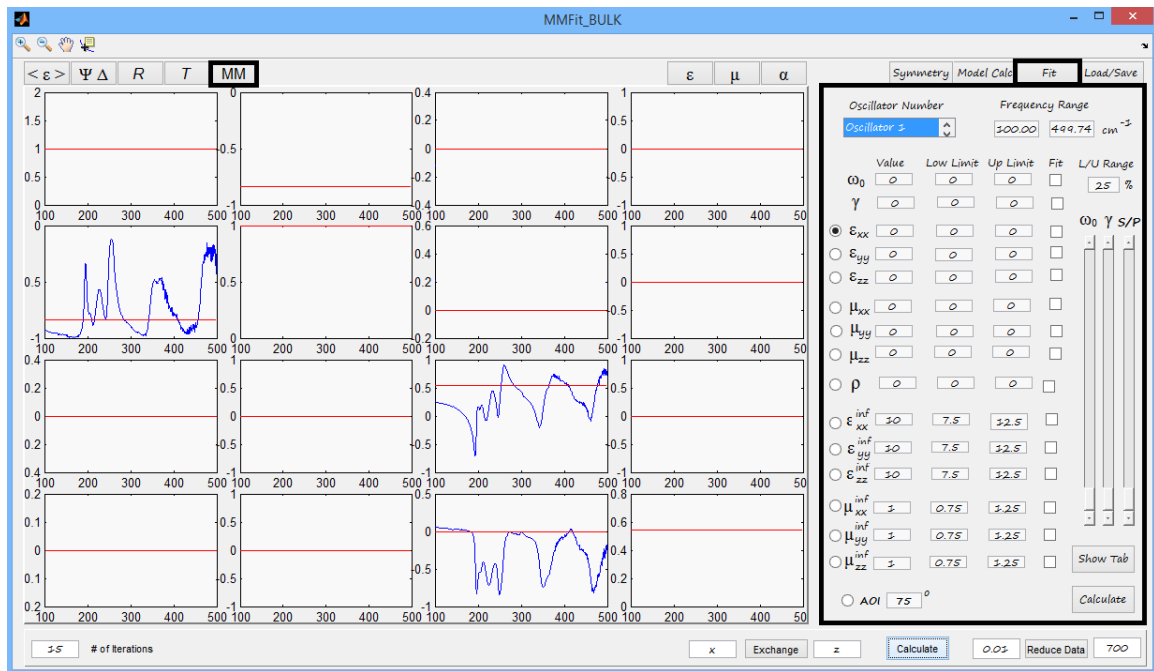


Figure 6.2 Load/Save panel in MMFit program after loading mmd format file and clicking on “MM Panel” button, containing three Mueller matrix components (m_{21}, m_{33}, m_{34}). Blue line – data. Red line – model.

There are 17 buttons on “Load/Save” panel. “Load *.mmd Data” allows user to load Mueller matrices data in mmd format. There are 16 non-normalized columns in mmd data file. MMFit normalize all MM components to the first MM component (first column).

```
* Start time : Wed 06/11/2014, 15:48:09
* Finish time : Wed 06/11/2014, 18:08:59
* OPUS data folder : \\Ellipse\Test data\2014 June\04 June TbFeO3
CxBy\opus
* The 1st OPUS data file : aaa.436
* The Last OPUS data file : aaa.491
* OPUS XPM file : \\Ellipse\Test data\2014 June\GeMy_700_1cm_512
_x8_100kHz.XPM
* Schedule file : \\Ellipse\Test data\2014 June\09 June TbFeO3
BxCy AOI 70 80\TBFeO3 BXCy MUELLER T DEP.sch
* Operator : Taras and Andrei
* Comments : DyFeO3
theta      2.680e+01
2theta     060
chi        014
X          000
Y          9.400e+00
Z          -4.000e-01
SetT       7.500e+00
T1         7.436e+00
T2         7.357e+00
B          000
#Mueller:
0.00000E+00  0.001767  0.000839  -0.000481  -0.000141
             0.001092  0.000531  -0.000869  -0.000234  0.000026
             -0.000142 -0.001300  -0.000232  0.000113  0.000160
             0.000114  -0.000733
4.82116E-01  0.000859  0.000685  -0.000355  -0.000220
             0.000970  0.000312  -0.000749  -0.000272  -0.000112
             0.000138  -0.001097  0.000117  -0.000024  0.000147
             0.000192  -0.000831
9.64233E-01  0.000684  -0.000092  0.000110  -0.000114
             0.000329  -0.000090  0.000199  -0.000115  -0.000041
```

Figure 6.3 MMD data file structure.

“Load *.epd Data” button allows user to load data in epd format, containing real part of pseudo-dielectric function (column six), imaginary part of pseudo-dielectric function (column seven), Ψ function (column two), Δ function (column three). Mmd and epd data formats are shown in Figures 6.3,6.4 correspondingly.

```

mAB2PD 2013-01-23 14:04:41 E:\EllipsometerData\January 2013
\01152013\SAMP TEST2 AOI 75 ALPHA2=(20 T=300+-20 T=300+25 T=300
+-25 T=300+30 T=300+-30 T=300+40 T=300+-40 T=300+45 T=300+-45 T=
300).big "STO"
Phi=75.00deg Po=(-2.83 ± 0.013)deg Ao=(2.81 ± 0.02)deg
corr.coef.=-0.23 Pflip=30.00deg E-calib(80, 650)1/cm
Comments:
wn[cm-1], Psi[deg] , Delta[deg], dPsi[deg] ,dDelta[deg],
Epsilon1 , Epsilon2 , dEpsilon1 , dEpsilon2
70 12.110909 -0.51889921 12.110909 -0.51889921
12.110909 -0.51889921
70.5 11.636195 -1.0725924 11.636195 -1.0725924 11.636195
-1.0725924
71 12.684736 -2.1213488 12.684736 -2.1213488 12.684736
-2.1213488
71.5 14.393121 -3.3437035 14.393121 -3.3437035 14.393121
-3.3437035
72 15.600339 -4.2315141 15.600339 -4.2315141 15.600339
-4.2315141
72.5 16.198761 -4.5870295 16.198761 -4.5870295 16.198761
-4.5870295
73 16.713629 -4.4454636 16.713629 -4.4454636 16.713629
-4.4454636
73.5 17.215107 -3.9070955 17.215107 -3.9070955 17.215107
-3.9070955
74 17.574487 -3.2138467 17.574487 -3.2138467 17.574487
-3.2138467
74.5 17.847448 -2.669105 17.847448 -2.669105 17.847448
-2.669105
75 17.739289 -2.372324 17.739289 -2.372324 17.739289
-2.372324
75.5 16.820506 -2.1473462 16.820506 -2.1473462 16.820506
-2.1473462

```

Figure 6.4 EPD data file structure.

Following twelve buttons allow user to load separately pseudo-dielectric function data, Ψ function data, Δ function data, reflection data, transmission data. Data files must contain two columns only without any headers. First column should be frequency in inverse centimeters, second column is intensity data. If one loads pseudo-dielectric function data using “Load *.epd Data” and then load another pseudo-dielectric function data using “Load <Eps1> Data” and/or “Load <Eps2> Data”, corresponding data will be rewritten to the newest one. This works for Ψ and Δ functions data as well.

“Reduce Data” button on the lower panel allows to cut data in the defined by user range”. To restore data original data file should be loaded and reduced data will be rewritten to the new one.

“Load Project” button allows to load project previously saved by “Save Project” button. “Save Project” button gives overall saving option: all available data, models and parameters will be recorded.

“Save FitData” button saves all models and all data to separate files, consisting of two columns: first one is frequency, second one is intensity. If there were no loaded data previously, MMFit programs provides file with zero data. The same is valid for models. Total number of files saved after “Save FitData” button clicked is 25.

6.2 Working with Models

For creation and modifying model function user should click on “Model Calc” button in the right panel.

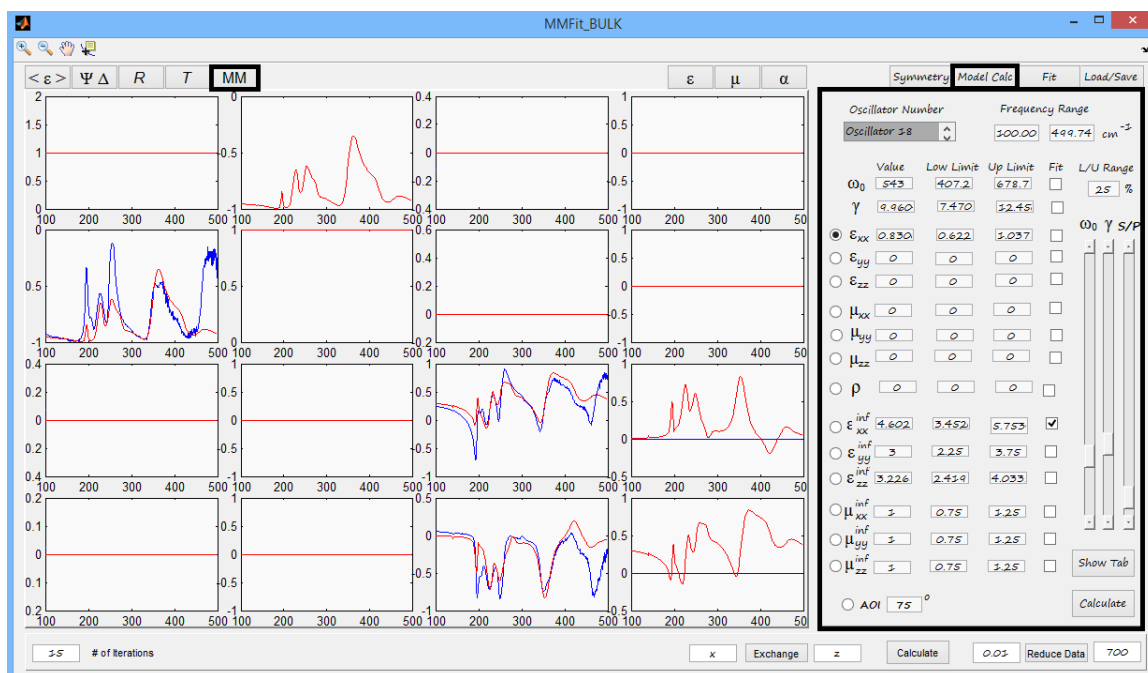


Figure 6.5 “Model Calc” panel with “MM” data panel after creating rough starting model for fitting. Blue line – data. Red line – model.

There are three sliders available for adjusting different values. First slider (from the left to the right) always changes oscillation frequency value. Second slider always changes Gamma (broadening coefficient) value. Third slider changes value chosen by radiobuttons. When one changes values with sliders current models are redrawn dynamically. Main purpose of this visualization is to find starting fitting point maximally close to the original data.

“Show Tab” button draws additional panel which gives overall picture of the

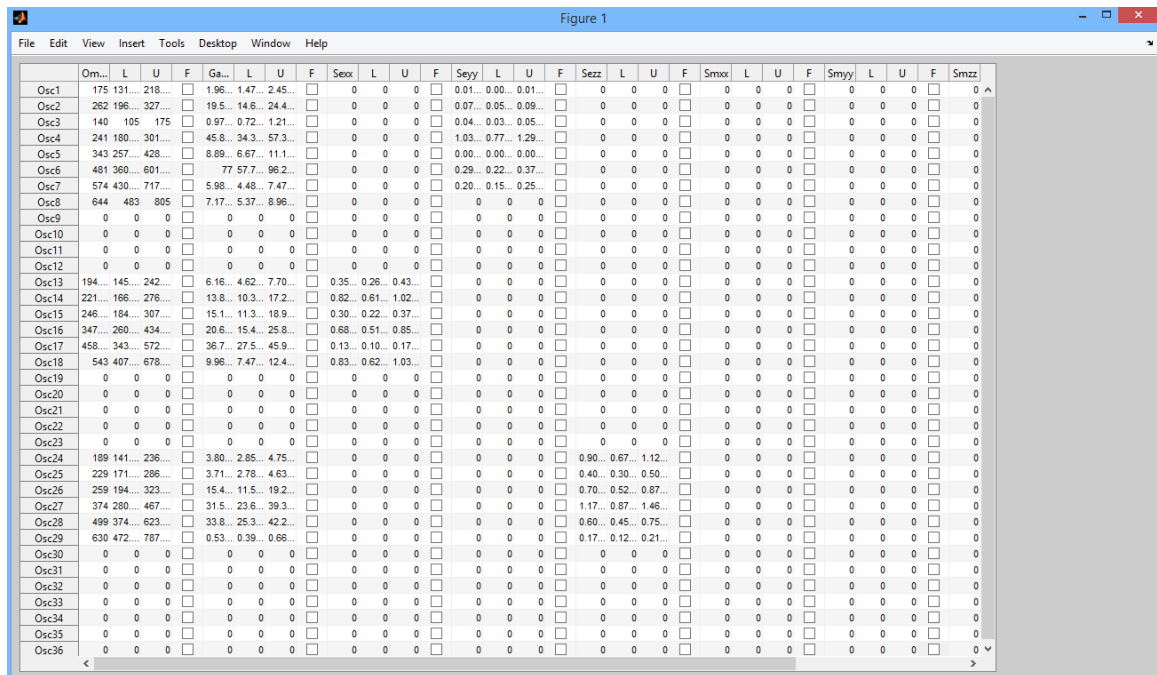


Figure 6.6 “Show Tab” panel view with model parameters.

current model. User has option to change available values from this panel as well. After adjusting all values additional click on free space should be made and current window should be closed. “L” stands for low fitting boundary. “U” stands for high fitting boundary. “F” stands for fit. If some value is supposed to be fitted, one should mark corresponding checkbox. When checkbox is chosen, “L” and “U” values are updated automatically by

\pm value from “L/U Range” edit field percent from the initial value of current parameter.

“Fitting Range” allows to choose appropriate range in inverse centimeters for fitting.

In order to choose ME tensor symmetry or add off diagonal components of electric permittivity tensor user should click on “Symmetry” button in the right panel.

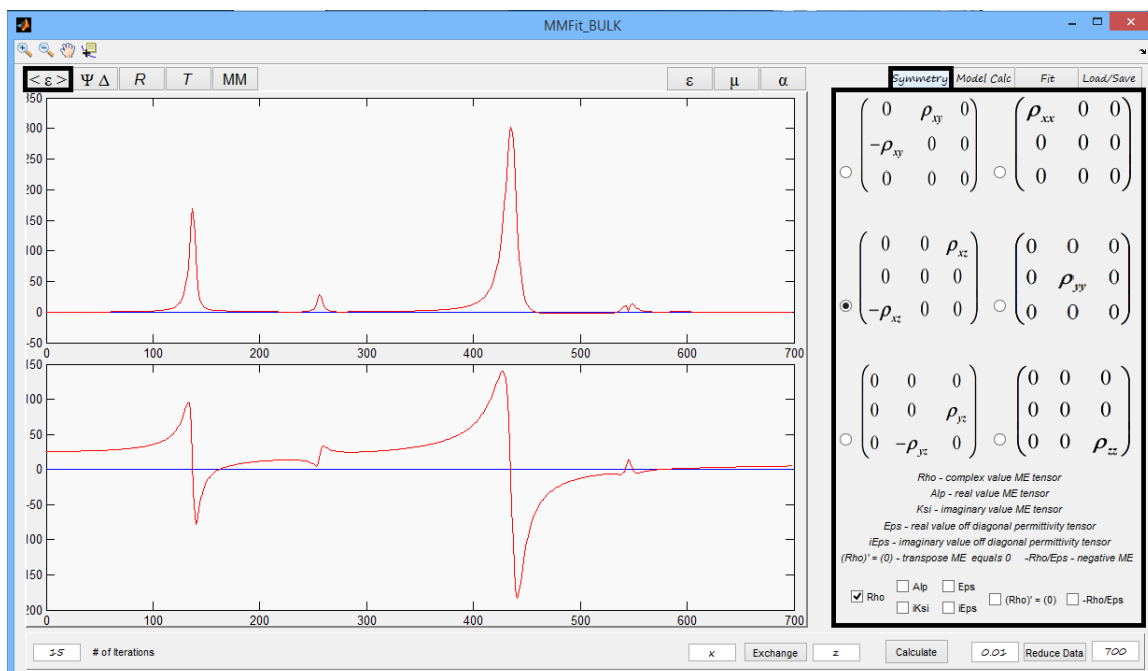


Figure 6.7 “Symmetry” panel view and pseudo-dielectric function data panel with model containing ME oscillator at 545 cm⁻¹.

There are six available options to construct ME tensor which are shown in Figure 6.7. Checkboxes in the low part of the panel allows to choose different options for ME tensor. “Rho” checkbox makes component of ME tensor complex , “Alp” checkbox makes them real, “Ksi” checkbox makes them purely imaginary, “Eps” makes ME tensor 0 and add corresponding real components to electric permittivity tensor. It should be noted that for this choice only off diagonal components available.”iEps” does the same as “Eps” but makes components purely imaginary.”Rho’ = 0” make transpose ME tensor 0

and “-Rho/Eps” makes negative ME tensor or if “Eps”, “iEps” options are chosen makes negative off diagonal terms of permittivity tensor.

After model is constructed clicking on “Calculate ” button plots model in the left panel for all functions. There is “Calculate ” button on the lower panel and on the “Model Calc” panel as well.

6.3 Working with Fitting

In this section fitting options are explained.

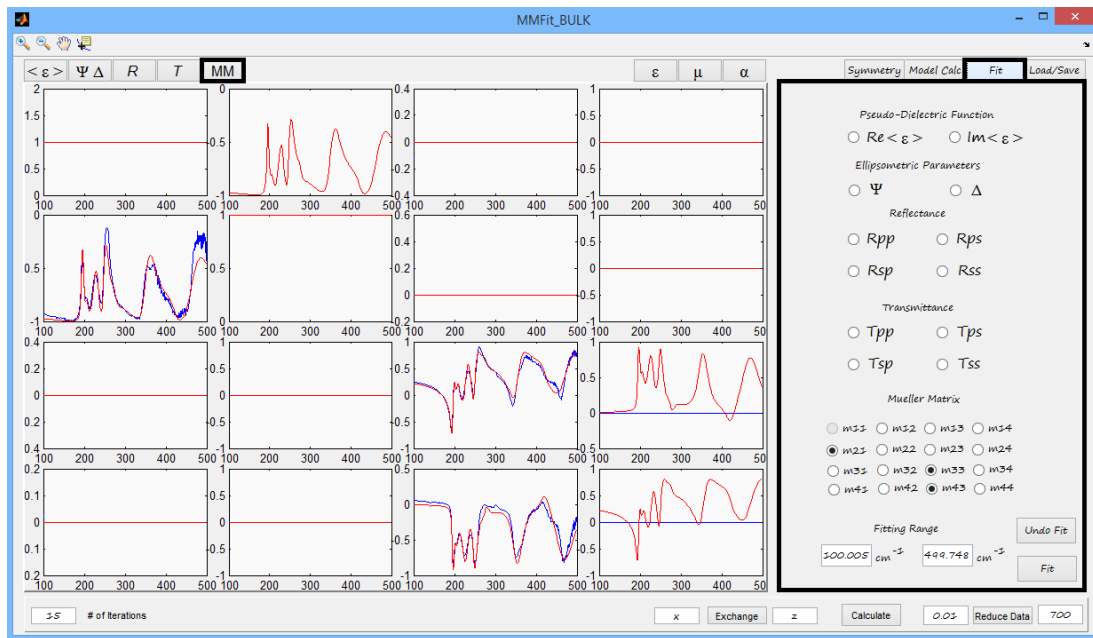


Figure 6.8 “Fitting” panel view with “MM” data panel after fitting three Mueller matrix components. Blue line – data. Red line – model.

“Fit” panel allows to choose different set of data for simultaneous fitting. Desired data for fit should be marked by means of radio buttons. After choosing appropriate sets of data fitting frequency boundaries could be adjusted in “Fitting range Field”. “Fit” button starts fitting procedure. After fit is finished, fitted values are renewed. Left edit box in the low panel allows to adjust number of fitting iterations.

CHAPTER 5

SUMMARY

In this Thesis we accomplished the following research objectives:

- Analysis of numerical and analytical methods for electromagnetic wave propagation in bi-anisotropic media has been done.
- Analytical expressions for Fresnel's coefficients have been derived for bi-anisotropic bulk and multilayer materials.
- Based on obtained theoretical results the original data fitting and simulation software have been developed.
- IR spectra of Dy-IG and TbMnO₃ multiferroics have been analyzed and their parameters such as frequencies and oscillator strengths have been determined.
- Infrared active optical phonons in hexagonal rare earth manganites have been studied. A systematic variation of the phonon frequencies vs. the rare earth ion mass and rare earth ion radius has been observed in *RMnO₃* compounds.

A logical continuation of the current research should be focused on the experimental observation of the optical properties for new materials with predicted magneto-electric interaction. Interesting behavior of such samples is expected under application of external magnetic and electric fields. Correspondingly, the developed theoretical formalism should be extended for cases with applied external fields. For thin film structures, which are suitable for different applications in industry and technology, interlayer interaction of ME oscillations is under considerable interest and should be studied in more details using Mueller matrix ellipsometry.

APPENDIX A

$\tilde{\Delta}$ MATRIX EIGENVALUES EXPLICIT FORMULAS

In this appendix general formulas are given for eigenvalues of arbitrary structure $\tilde{\Delta}$ matrix which is in the form

$$\tilde{\Delta} = \begin{pmatrix} \Delta_{11} & \Delta_{12} & \Delta_{13} & \Delta_{14} \\ \Delta_{21} & \Delta_{22} & \Delta_{23} & \Delta_{24} \\ \Delta_{31} & \Delta_{32} & \Delta_{33} & \Delta_{34} \\ \Delta_{41} & \Delta_{42} & \Delta_{43} & \Delta_{44} \end{pmatrix} \quad (5.1)$$

For the most general case when the symmetry of ME tensor is the lowest, optical matrix and $\tilde{\Delta}$ matrix have the following forms:

$$M = \begin{pmatrix} \varepsilon_{xx} & 0 & 0 & \alpha_{xx} & \alpha_{xy} & \alpha_{xz} \\ 0 & \varepsilon_{yy} & 0 & \alpha_{yx} & \alpha_{yy} & \alpha_{yz} \\ 0 & 0 & \varepsilon_{zz} & \alpha_{zx} & \alpha_{zy} & \alpha_{zz} \\ \alpha'_{xx} & \alpha'_{yx} & \alpha'_{zx} & \mu_{xx} & 0 & 0 \\ \alpha'_{xy} & \alpha'_{yy} & \alpha'_{zy} & 0 & \mu_{yy} & 0 \\ \alpha'_{xz} & \alpha'_{yz} & \alpha'_{zz} & 0 & 0 & \mu_{zz} \end{pmatrix} \quad (5.2)$$

$$\tilde{\Delta} = \begin{pmatrix} \alpha'_{xy} + \frac{\alpha_{zz}\alpha'_{xz}(\alpha'_{zy} + q_x)}{\varepsilon_{zz}\mu_{zz} - \alpha_{zz}\alpha'_{zz}} & \alpha'_{yy} + \frac{\alpha_{zz}(\alpha'_{yz} - q_x)(\alpha'_{zy} + q_x)}{\varepsilon_{zz}\mu_{zz} - \alpha_{zz}\alpha'_{zz}} & -\frac{\mu_{zz}\alpha_{zx}(\alpha'_{zy} + q_x)}{\varepsilon_{zz}\mu_{zz} - \alpha_{zz}\alpha'_{zz}} & \mu_{yy} - \frac{\mu_{zz}(\alpha_{zy} + q_x)(\alpha'_{zy} + q_x)}{\varepsilon_{zz}\mu_{zz} - \alpha_{zz}\alpha'_{zz}} \\ -\alpha'_{xx} - \frac{(\alpha_{zz}\alpha'_{xz}\alpha'_{zx})}{\varepsilon_{zz}\mu_{zz} - \alpha_{zz}\alpha'_{zz}} & -\alpha'_{yx} - \frac{\alpha_{zz}\alpha'_{zx}(\alpha'_{yz} - q_x)}{\varepsilon_{zz}\mu_{zz} - \alpha_{zz}\alpha'_{zz}} & \frac{\mu_{zz}\alpha_{zx}\alpha'_{zx}}{\varepsilon_{zz}\mu_{zz} - \alpha_{zz}\alpha'_{zz}} - \mu_{xx} & -\frac{\mu_{zz}(\alpha_{zy} + q_x)\alpha'_{zx}}{\varepsilon_{zz}\mu_{zz} - \alpha_{zz}\alpha'_{zz}} \\ \frac{\varepsilon_{zz}\alpha'_{xz}(\alpha_{yz} - q_x)}{\varepsilon_{zz}\mu_{zz} - \alpha_{zz}\alpha'_{zz}} & \frac{\varepsilon_{zz}(\alpha'_{yz} - q_x)(\alpha_{yz} - q_x)}{\varepsilon_{zz}\mu_{zz} - \alpha_{zz}\alpha'_{zz}} - \varepsilon_{yy} & -\alpha'_{yx} - \frac{\alpha'_{zz}\alpha_{zx}(\alpha_{yz} - q_x)}{\varepsilon_{zz}\mu_{zz} - \alpha_{zz}\alpha'_{zz}} & -\alpha'_{yy} - \frac{\alpha'_{zz}(\alpha_{zy} - q_x)(\alpha_{zy} + q_x)}{\varepsilon_{zz}\mu_{zz} - \alpha_{zz}\alpha'_{zz}} \\ \varepsilon_{xx} - \frac{\varepsilon_{zz}\alpha_{xz}\alpha'_{xz}}{\varepsilon_{zz}\mu_{zz} - \alpha_{zz}\alpha'_{zz}} & -\frac{\varepsilon_{zz}\alpha_{xz}(\alpha'_{yz} - q_x)}{\varepsilon_{zz}\mu_{zz} - \alpha_{zz}\alpha'_{zz}} & \alpha_{xx} + \frac{\alpha'_{zz}\alpha_{zx}\alpha_{xz}}{\varepsilon_{zz}\mu_{zz} - \alpha_{zz}\alpha'_{zz}} & -\alpha_{xy} - \frac{\alpha'_{zz}\alpha_{xz}(\alpha_{zy} + q_x)}{\varepsilon_{zz}\mu_{zz} - \alpha_{zz}\alpha'_{zz}} \end{pmatrix} \quad (5.3)$$

Components of $\tilde{\Delta}$ matrix can be extracted from Equation (5.3). Earlier we pointed out that in order to resolve eigenvalue problem we need to extract solutions of fourth order polynomial in the form Equation (3.22), where C_1, C_2, C_3, C_4 can be found from the condition

$$\det \begin{pmatrix} \Delta_{11} - q_{z,i} & \Delta_{12} & \Delta_{13} & \Delta_{14} \\ \Delta_{21} & \Delta_{22} - q_{z,i} & \Delta_{23} & \Delta_{24} \\ \Delta_{31} & \Delta_{32} & \Delta_{33} - q_{z,i} & \Delta_{34} \\ \Delta_{41} & \Delta_{42} & \Delta_{43} & \Delta_{44} - q_{z,i} \end{pmatrix} = 0,$$

with solutions:

$$C_1 = -\Delta_{11} - \Delta_{22} - \Delta_{33} - \Delta_{44}$$

$$C_2 = -\Delta_{12}\Delta_{21} + \Delta_{11}\Delta_{22} - \Delta_{13}\Delta_{31} - \Delta_{23}\Delta_{32} + \Delta_{11}\Delta_{33} + \Delta_{22}\Delta_{33} - \Delta_{14}\Delta_{41} - \Delta_{24}\Delta_{42} - \Delta_{34}\Delta_{43} + \Delta_{11}\Delta_{44} + \Delta_{22}\Delta_{44} + \Delta_{33}\Delta_{44}$$

$$C_3 = \Delta_{13}\Delta_{22}\Delta_{31} - \Delta_{12}\Delta_{23}\Delta_{31} - \Delta_{13}\Delta_{21}\Delta_{32} + \Delta_{11}\Delta_{23}\Delta_{32} + \Delta_{12}\Delta_{21}\Delta_{33} - \Delta_{11}\Delta_{22}\Delta_{33} + \Delta_{14}\Delta_{22}\Delta_{41} - \Delta_{12}\Delta_{24}\Delta_{41} + \Delta_{14}\Delta_{33}\Delta_{41} - \Delta_{13}\Delta_{34}\Delta_{41} - \Delta_{14}\Delta_{21}\Delta_{42} + \Delta_{11}\Delta_{24}\Delta_{42} + \Delta_{24}\Delta_{33}\Delta_{42} - \Delta_{23}\Delta_{34}\Delta_{42} - \Delta_{14}\Delta_{31}\Delta_{43} - \Delta_{24}\Delta_{32}\Delta_{43} + \Delta_{11}\Delta_{34}\Delta_{43} + \Delta_{22}\Delta_{34}\Delta_{43} + \Delta_{12}\Delta_{21}\Delta_{44} - \Delta_{11}\Delta_{22}\Delta_{44} + \Delta_{13}\Delta_{31}\Delta_{44} + \Delta_{23}\Delta_{32}\Delta_{44} - \Delta_{11}\Delta_{33}\Delta_{44} - \Delta_{22}\Delta_{33}\Delta_{44}$$

$$C_4 = \Delta_{14}\Delta_{23}\Delta_{32}\Delta_{41} - \Delta_{13}\Delta_{24}\Delta_{32}\Delta_{41} - \Delta_{14}\Delta_{22}\Delta_{33}\Delta_{41} + \Delta_{12}\Delta_{24}\Delta_{33}\Delta_{41} + \Delta_{13}\Delta_{22}\Delta_{34}\Delta_{41} - \Delta_{12}\Delta_{23}\Delta_{34}\Delta_{41} - \Delta_{14}\Delta_{23}\Delta_{31}\Delta_{42} + \Delta_{13}\Delta_{24}\Delta_{31}\Delta_{42} + \Delta_{14}\Delta_{21}\Delta_{33}\Delta_{42} - \Delta_{11}\Delta_{24}\Delta_{33}\Delta_{42} - \Delta_{13}\Delta_{21}\Delta_{34}\Delta_{42} + \Delta_{11}\Delta_{23}\Delta_{34}\Delta_{42} + \Delta_{14}\Delta_{22}\Delta_{31}\Delta_{43} - \Delta_{14}\Delta_{21}\Delta_{32}\Delta_{43} + \Delta_{11}\Delta_{24}\Delta_{32}\Delta_{43} - \Delta_{11}\Delta_{22}\Delta_{34}\Delta_{43} - \Delta_{12}(\Delta_{24}\Delta_{31} - \Delta_{21}\Delta_{34})\Delta_{43}$$

and $q_{z,i}$ is one of the four eigenvalues of $\tilde{\Delta}$ matrix. Eigenvalues formulas are given

below (discussion of universal method for solving quartic equation and analytical

solutions are given in [15]):

$$\begin{aligned}
q_{z,1} = & -\frac{C_1}{4} - \frac{1}{2} \sqrt{\left(\frac{C_1^2}{4} - \frac{2C_2}{3} + \frac{2^{1/3} (C_2^2 - 3C_1C_3 + 12C_4)}{3 \left(2C_2^3 - 9C_1C_2C_3 + 27C_3^2 + 27C_1^2C_4 - 72C_2C_4 + \sqrt{-4(C_2^2 - 3C_1C_3 + 12C_4)^3 + (2C_2^3 - 9C_1C_2C_3 + 27C_3^2 + 27C_1^2C_4 - 72C_2C_4)^2} \right)^{1/3}} + \right. \\
& \left. \frac{\left(2C_2^3 - 9C_1C_2C_3 + 27C_3^2 + 27C_1^2C_4 - 72C_2C_4 + \sqrt{-4(C_2^2 - 3C_1C_3 + 12C_4)^3 + (2C_2^3 - 9C_1C_2C_3 + 27C_3^2 + 27C_1^2C_4 - 72C_2C_4)^2} \right)^{1/3}}{3 \times 2^{1/3}} \right) - \\
& \frac{1}{2} \sqrt{\left(\frac{C_1^2}{2} - \frac{4C_2}{3} - \frac{2^{1/3} (C_2^2 - 3C_1C_3 + 12C_4)}{3 \left(2C_2^3 - 9C_1C_2C_3 + 27C_3^2 + 27C_1^2C_4 - 72C_2C_4 + \sqrt{-4(C_2^2 - 3C_1C_3 + 12C_4)^3 + (2C_2^3 - 9C_1C_2C_3 + 27C_3^2 + 27C_1^2C_4 - 72C_2C_4)^2} \right)^{1/3}} - \right. \\
& \left. \frac{\left(2C_2^3 - 9C_1C_2C_3 + 27C_3^2 + 27C_1^2C_4 - 72C_2C_4 + \sqrt{-4(C_2^2 - 3C_1C_3 + 12C_4)^3 + (2C_2^3 - 9C_1C_2C_3 + 27C_3^2 + 27C_1^2C_4 - 72C_2C_4)^2} \right)^{1/3}}{3 \times 2^{1/3}} \right) - \\
& (-C_1^3 + 4C_1C_2 - 8C_3) / \\
& \left(4 \sqrt{\left(\frac{C_1^2}{4} - \frac{2C_2}{3} + \frac{2^{1/3} (C_2^2 - 3C_1C_3 + 12C_4)}{3 \left(2C_2^3 - 9C_1C_2C_3 + 27C_3^2 + 27C_1^2C_4 - 72C_2C_4 + \sqrt{-4(C_2^2 - 3C_1C_3 + 12C_4)^3 + (2C_2^3 - 9C_1C_2C_3 + 27C_3^2 + 27C_1^2C_4 - 72C_2C_4)^2} \right)^{1/3}} + \right. \right. \\
& \left. \left. \frac{\left(2C_2^3 - 9C_1C_2C_3 + 27C_3^2 + 27C_1^2C_4 - 72C_2C_4 + \sqrt{-4(C_2^2 - 3C_1C_3 + 12C_4)^3 + (2C_2^3 - 9C_1C_2C_3 + 27C_3^2 + 27C_1^2C_4 - 72C_2C_4)^2} \right)^{1/3}}{3 \times 2^{1/3}} \right) \right) \right),
\end{aligned}$$

$$\begin{aligned}
q_{z,2} = & -\frac{C_1}{4} - \frac{1}{2} \sqrt{\left(\frac{C_1^2}{4} - \frac{2C_2}{3} + \frac{2^{1/3} (C_2^2 - 3C_1C_3 + 12C_4)}{3 \left(2C_2^3 - 9C_1C_2C_3 + 27C_3^2 + 27C_1^2C_4 - 72C_2C_4 + \sqrt{-4(C_2^2 - 3C_1C_3 + 12C_4)^3 + (2C_2^3 - 9C_1C_2C_3 + 27C_3^2 + 27C_1^2C_4 - 72C_2C_4)^2} \right)^{1/3}} + \right. \\
& \left. \frac{\left(2C_2^3 - 9C_1C_2C_3 + 27C_3^2 + 27C_1^2C_4 - 72C_2C_4 + \sqrt{-4(C_2^2 - 3C_1C_3 + 12C_4)^3 + (2C_2^3 - 9C_1C_2C_3 + 27C_3^2 + 27C_1^2C_4 - 72C_2C_4)^2} \right)^{1/3}}{3 \times 2^{1/3}} \right) + \\
& \frac{1}{2} \sqrt{\left(\frac{C_1^2}{2} - \frac{4C_2}{3} - \frac{2^{1/3} (C_2^2 - 3C_1C_3 + 12C_4)}{3 \left(2C_2^3 - 9C_1C_2C_3 + 27C_3^2 + 27C_1^2C_4 - 72C_2C_4 + \sqrt{-4(C_2^2 - 3C_1C_3 + 12C_4)^3 + (2C_2^3 - 9C_1C_2C_3 + 27C_3^2 + 27C_1^2C_4 - 72C_2C_4)^2} \right)^{1/3}} - \right. \\
& \left. \frac{\left(2C_2^3 - 9C_1C_2C_3 + 27C_3^2 + 27C_1^2C_4 - 72C_2C_4 + \sqrt{-4(C_2^2 - 3C_1C_3 + 12C_4)^3 + (2C_2^3 - 9C_1C_2C_3 + 27C_3^2 + 27C_1^2C_4 - 72C_2C_4)^2} \right)^{1/3}}{3 \times 2^{1/3}} \right) - \\
& (-C_1^3 + 4C_1C_2 - 8C_3) / \\
& \left(4 \sqrt{\left(\frac{C_1^2}{4} - \frac{2C_2}{3} + \frac{2^{1/3} (C_2^2 - 3C_1C_3 + 12C_4)}{3 \left(2C_2^3 - 9C_1C_2C_3 + 27C_3^2 + 27C_1^2C_4 - 72C_2C_4 + \sqrt{-4(C_2^2 - 3C_1C_3 + 12C_4)^3 + (2C_2^3 - 9C_1C_2C_3 + 27C_3^2 + 27C_1^2C_4 - 72C_2C_4)^2} \right)^{1/3}} + \right. \right. \\
& \left. \left. \frac{\left(2C_2^3 - 9C_1C_2C_3 + 27C_3^2 + 27C_1^2C_4 - 72C_2C_4 + \sqrt{-4(C_2^2 - 3C_1C_3 + 12C_4)^3 + (2C_2^3 - 9C_1C_2C_3 + 27C_3^2 + 27C_1^2C_4 - 72C_2C_4)^2} \right)^{1/3}}{3 \times 2^{1/3}} \right) \right) \right),
\end{aligned}$$

$$\begin{aligned}
q_{z,3} = & -\frac{C_1}{4} + \frac{1}{2} \sqrt{\left(\frac{C_1^2}{4} - \frac{2C_2}{3} + \frac{2^{1/3} (C_2^2 - 3C_1C_3 + 12C_4)}{3 \left(2C_2^3 - 9C_1C_2C_3 + 27C_3^2 + 27C_1^2C_4 - 72C_2C_4 + \sqrt{-4(C_2^2 - 3C_1C_3 + 12C_4)^3 + (2C_2^3 - 9C_1C_2C_3 + 27C_3^2 + 27C_1^2C_4 - 72C_2C_4)^2} \right)^{1/3}} \right.} \\
& \left. \frac{\left(2C_2^3 - 9C_1C_2C_3 + 27C_3^2 + 27C_1^2C_4 - 72C_2C_4 + \sqrt{-4(C_2^2 - 3C_1C_3 + 12C_4)^3 + (2C_2^3 - 9C_1C_2C_3 + 27C_3^2 + 27C_1^2C_4 - 72C_2C_4)^2} \right)^{1/3}}{3 \times 2^{1/3}} \right) -} \\
& \frac{1}{2} \sqrt{\left(\frac{C_1^2}{2} - \frac{4C_2}{3} - \frac{2^{1/3} (C_2^2 - 3C_1C_3 + 12C_4)}{3 \left(2C_2^3 - 9C_1C_2C_3 + 27C_3^2 + 27C_1^2C_4 - 72C_2C_4 + \sqrt{-4(C_2^2 - 3C_1C_3 + 12C_4)^3 + (2C_2^3 - 9C_1C_2C_3 + 27C_3^2 + 27C_1^2C_4 - 72C_2C_4)^2} \right)^{1/3}} \right.} \\
& \left. \frac{\left(2C_2^3 - 9C_1C_2C_3 + 27C_3^2 + 27C_1^2C_4 - 72C_2C_4 + \sqrt{-4(C_2^2 - 3C_1C_3 + 12C_4)^3 + (2C_2^3 - 9C_1C_2C_3 + 27C_3^2 + 27C_1^2C_4 - 72C_2C_4)^2} \right)^{1/3}}{3 \times 2^{1/3}} \right) +} \\
& (-C_1^3 + 4C_1C_2 - 8C_3) / \\
& \left(4 \sqrt{\left(\frac{C_1^2}{4} - \frac{2C_2}{3} + \frac{2^{1/3} (C_2^2 - 3C_1C_3 + 12C_4)}{3 \left(2C_2^3 - 9C_1C_2C_3 + 27C_3^2 + 27C_1^2C_4 - 72C_2C_4 + \sqrt{-4(C_2^2 - 3C_1C_3 + 12C_4)^3 + (2C_2^3 - 9C_1C_2C_3 + 27C_3^2 + 27C_1^2C_4 - 72C_2C_4)^2} \right)^{1/3}} \right.} \right. \\
& \left. \left. \frac{\left(2C_2^3 - 9C_1C_2C_3 + 27C_3^2 + 27C_1^2C_4 - 72C_2C_4 + \sqrt{-4(C_2^2 - 3C_1C_3 + 12C_4)^3 + (2C_2^3 - 9C_1C_2C_3 + 27C_3^2 + 27C_1^2C_4 - 72C_2C_4)^2} \right)^{1/3}}{3 \times 2^{1/3}} \right) \right) \right),
\end{aligned}$$

$$\begin{aligned}
q_{z,4} = & -\frac{C_1}{4} + \frac{1}{2} \sqrt{\left(\frac{C_1^2}{4} - \frac{2C_2}{3} + \frac{2^{1/3} (C_2^2 - 3C_1C_3 + 12C_4)}{3 \left(2C_2^3 - 9C_1C_2C_3 + 27C_3^2 + 27C_1^2C_4 - 72C_2C_4 + \sqrt{-4(C_2^2 - 3C_1C_3 + 12C_4)^3 + (2C_2^3 - 9C_1C_2C_3 + 27C_3^2 + 27C_1^2C_4 - 72C_2C_4)^2} \right)^{1/3}} \right.} \\
& \left. \frac{\left(2C_2^3 - 9C_1C_2C_3 + 27C_3^2 + 27C_1^2C_4 - 72C_2C_4 + \sqrt{-4(C_2^2 - 3C_1C_3 + 12C_4)^3 + (2C_2^3 - 9C_1C_2C_3 + 27C_3^2 + 27C_1^2C_4 - 72C_2C_4)^2} \right)^{1/3}}{3 \times 2^{1/3}} \right) +} \\
& \frac{1}{2} \sqrt{\left(\frac{C_1^2}{2} - \frac{4C_2}{3} - \frac{2^{1/3} (C_2^2 - 3C_1C_3 + 12C_4)}{3 \left(2C_2^3 - 9C_1C_2C_3 + 27C_3^2 + 27C_1^2C_4 - 72C_2C_4 + \sqrt{-4(C_2^2 - 3C_1C_3 + 12C_4)^3 + (2C_2^3 - 9C_1C_2C_3 + 27C_3^2 + 27C_1^2C_4 - 72C_2C_4)^2} \right)^{1/3}} \right.} \\
& \left. \frac{\left(2C_2^3 - 9C_1C_2C_3 + 27C_3^2 + 27C_1^2C_4 - 72C_2C_4 + \sqrt{-4(C_2^2 - 3C_1C_3 + 12C_4)^3 + (2C_2^3 - 9C_1C_2C_3 + 27C_3^2 + 27C_1^2C_4 - 72C_2C_4)^2} \right)^{1/3}}{3 \times 2^{1/3}} \right) +} \\
& (-C_1^3 + 4C_1C_2 - 8C_3) / \\
& \left(4 \sqrt{\left(\frac{C_1^2}{4} - \frac{2C_2}{3} + \frac{2^{1/3} (C_2^2 - 3C_1C_3 + 12C_4)}{3 \left(2C_2^3 - 9C_1C_2C_3 + 27C_3^2 + 27C_1^2C_4 - 72C_2C_4 + \sqrt{-4(C_2^2 - 3C_1C_3 + 12C_4)^3 + (2C_2^3 - 9C_1C_2C_3 + 27C_3^2 + 27C_1^2C_4 - 72C_2C_4)^2} \right)^{1/3}} \right.} \right. \\
& \left. \left. \frac{\left(2C_2^3 - 9C_1C_2C_3 + 27C_3^2 + 27C_1^2C_4 - 72C_2C_4 + \sqrt{-4(C_2^2 - 3C_1C_3 + 12C_4)^3 + (2C_2^3 - 9C_1C_2C_3 + 27C_3^2 + 27C_1^2C_4 - 72C_2C_4)^2} \right)^{1/3}}{3 \times 2^{1/3}} \right) \right) \right).
\end{aligned}$$

Thus we found solutions for eigenvalues in terms of $\tilde{\Delta}$ matrix components. MatLab m-files with solutions can be found at [Error! Bookmark not defined.].

APPENDIX B

$\tilde{\Delta}$ MATRIX EIGENVECTORS EXPLICIT FORMULAS

In this appendix we find eigenvectors representation of $\tilde{\Delta}$ matrix. In order to get solutions we need to consider the following equation:

$$\begin{pmatrix} \Delta_{11} - q_{z,i} & \Delta_{12} & \Delta_{13} & \Delta_{14} \\ \Delta_{21} & \Delta_{22} - q_{z,i} & \Delta_{23} & \Delta_{24} \\ \Delta_{31} & \Delta_{32} & \Delta_{33} - q_{z,i} & \Delta_{34} \\ \Delta_{41} & \Delta_{42} & \Delta_{43} & \Delta_{44} - q_{z,i} \end{pmatrix} \begin{pmatrix} E_x \\ E_y \\ H_x \\ H_y \end{pmatrix} = 0 \quad (6.1)$$

where $q_{z,i}$ is one of the four eigenvalues of $\tilde{\Delta}$ matrix and their analytical solutions are given in Appendix A. Let's rewrite Equation (6.1) in the following form:

$$\begin{cases} (\Delta_{11} - q_{z,i})E_x + \Delta_{12}E_y + \Delta_{13}H_x + \Delta_{14}H_y = 0 \\ \Delta_{21}E_x + (\Delta_{22} - q_{z,i})E_y + \Delta_{23}H_x + \Delta_{24}H_y = 0 \\ \Delta_{31}E_x + \Delta_{32}E_y + (\Delta_{33} - q_{z,i})H_x + \Delta_{34}H_y = 0 \\ \Delta_{41}E_x + \Delta_{42}E_y + \Delta_{43}H_x + (\Delta_{44} - q_{z,i})H_y = 0. \end{cases} \quad (6.2)$$

Equation (6.2) is a linear system with respect to the tangential field components. It's not hard to show that general solution for each out of four possible eigenvectors has the structure shown below:

$$\begin{pmatrix} \psi_{1,i} \\ \psi_{2,i} \\ \psi_{3,i} \\ \psi_{4,i} \end{pmatrix} = \begin{pmatrix} E_x \\ E_y \\ H_x \\ H_y \end{pmatrix}_{eigen, q_{z,i}} = \begin{pmatrix} \frac{\Delta_{12}(-\Delta_{23}\Delta_{34} + \Delta_{24}(\Delta_{33} - q_{z,i})) - \Delta_{13}(\Delta_{24}\Delta_{32} + \Delta_{34}(-\Delta_{22} + q_{z,i})) + \Delta_{14}(\Delta_{23}\Delta_{32} + (\Delta_{22} - q_{z,i})(-\Delta_{33} + q_{z,i}))}{(-\Delta_{23}\Delta_{32} + (\Delta_{22} - q_{z,i})(\Delta_{33} - q_{z,i}))(\Delta_{11} - q_{z,i}) + \Delta_{13}(\Delta_{21}\Delta_{32} + \Delta_{31}(-\Delta_{22} + q_{z,i})) + \Delta_{12}(\Delta_{23}\Delta_{31} + \Delta_{21}(-\Delta_{33} + q_{z,i}))} \\ \frac{\Delta_{13}(-\Delta_{24}\Delta_{31} + \Delta_{21}\Delta_{34}) + \Delta_{14}(\Delta_{23}\Delta_{31} + \Delta_{21}(-\Delta_{33} + q_{z,i})) - (\Delta_{11} - q_{z,i})(\Delta_{23}\Delta_{34} + \Delta_{24}(-\Delta_{33} + q_{z,i}))}{(-\Delta_{23}\Delta_{32} + (\Delta_{22} - q_{z,i})(\Delta_{33} - q_{z,i}))(\Delta_{11} - q_{z,i}) + \Delta_{13}(\Delta_{21}\Delta_{32} + \Delta_{31}(-\Delta_{22} + q_{z,i})) + \Delta_{12}(\Delta_{23}\Delta_{31} + \Delta_{21}(-\Delta_{33} + q_{z,i}))} \\ \frac{\Delta_{12}(-\Delta_{24}\Delta_{31} + \Delta_{21}\Delta_{34}) + \Delta_{14}(-\Delta_{21}\Delta_{32} + \Delta_{31}(\Delta_{22} - q_{z,i})) + (\Delta_{11} - q_{z,i})(\Delta_{24}\Delta_{32} + \Delta_{34}(-\Delta_{22} + q_{z,i}))}{(-\Delta_{23}\Delta_{32} + (\Delta_{22} - q_{z,i})(\Delta_{33} - q_{z,i}))(\Delta_{11} - q_{z,i}) + \Delta_{13}(\Delta_{21}\Delta_{32} + \Delta_{31}(-\Delta_{22} + q_{z,i})) + \Delta_{12}(\Delta_{23}\Delta_{31} + \Delta_{21}(-\Delta_{33} + q_{z,i}))} \\ \frac{\Delta_{23}\Delta_{31} + \Delta_{21}(-\Delta_{33} + q_{z,i})}{1} \end{pmatrix} \quad (6.3)$$

In Equation (6.3) eigenvector components are normalized by H_y . In previous appendix A we showed explicit solutions for eigenvalues. That means eigenvectors problem is solved completely. Due to a very bulky structure of formulas in terms of optical parameters such as $\varepsilon, \mu, \alpha, AOI$, etc., we don't show final results here, though they are available in MatLab m-functions.

APPENDIX C
DOUBLE LAYER STRUCTURE PARTIAL TRANSFER MATRIX
REPRESENTATION

In Chapter 3 on electromagnetic waves propagation in multilayer structures we showed that partial transfer matrix can be written in the form of Equation (3.19) with β coefficients in the form of Equation (3.20). We present transfer matrix formulas for bilayer structure below:

[illegible]

$$T_{23} =$$

[illegible]

$$T_{24} =$$

[illegible]

REFERENCES

-
- [1] J. B. Pendry, Negative refraction, Contemporary Physics 45, 191 (2004).
 - [2] N.A.Spaldin, S.Cheong, R. Ramesh “Multiferroics: Past, Present and Future,” Physics today, October (2010), pp 39-43
 - [3] D. W. Ward, E. Statz, K. J. Webb, and K. A. Nelson “The Role of Multiferroics in the Negative Index of Refraction,” January 1, (2004)
 - [4] V. G. Veselago, Electrodynamics of substances with simultaneously negative values of ϵ and μ , Soviet Physics USPEKHI 10, 509 (1968).
 - [5] R.A. Shelby, D.R. Smith, and S. Schultz, “Experimental Verification of a Negative Index of Refraction,” Science 292, 77-79 (2001).
 - [6] I. E. Dzyaloshinskii, “On the Magneto-Electrical Effect in Antiferromagnets”, Soviet Phys. JETP 10, 628 (1960).
 - [7] D.Berreman, J. Opt. Soc. Am. 62, 502 (1972)
 - [8] R. Azzam “ Ellipsometry and Polarized Light,” North Holland Publishing Company, (1977)
 - [9] P. D. Rogers, T. D. Kang, T. Zhou, M. Kotelyanskii, and A. A. Sirenko, “Mueller matrices for anisotropic metamaterials generated using 4×4 matrix formalism”, Thin Solid Films, Sept. (2010).
 - [10] P. D. Rogers “Analysis of Mueller Matrices of Metamaterials and Multiferroics,” May (2011), NJIT
 - [11] P. Yeh “Electromagnetic propagation in birefringent layered media,” J. Opt. Soc. Am., Vol.69, No. 5, May (1979)
 - [12] M. Schubert, Generalized ellipsometry and complex optical systems, Thin Solid Films 313]314 1998 323]332
 - [13] H. Wohler, M. Fritsch, G. Haas, and D. A. Mlynski, J.Opt. Soc.Am. A 5, 1554, 1988
 - [14] Abramowitz, Milton; Stegun, Irene A., eds. (1972), Handbook of Mathematical Functions with Formulas, Graphs, and Mathematical Tables, New York: Dover Publications, ISBN 978-0-486-61272-0
 - [15] S. L. Shmakov, A Universal Method of Solving Quartic Equation, International Journal of Pure and Applied Mathematics, Volume 71 No. 2 2011, 251-259